

Mechanistic insight into the cyclohexene epoxidation with VO(acac)₂ and *tert*-butyl hydroperoxide

Matthias Vandichel¹, Karen Leus², Pascal Van Der Voort², Michel Waroquier^{1,*} and Veronique Van Speybroeck^{1,*}

¹ Center for Molecular Modeling, Ghent University, Technologiepark 903, 9052 Zwijnaarde, Belgium

² Department of Inorganic and Physical Chemistry, Center for Ordered Materials, Organometallics and Catalysis, Ghent University, Krijgslaan 281 – building S3, 9000 Gent, Belgium

*Corresponding authors: Prof. M. Waroquier michel.waroquier@ugent.be, Prof. V. Van Speybroeck, veronique.vanspeybroeck@ugent.be.

Abstract

The epoxidation reaction of cyclohexene is investigated for the system vanadyl acetylacetonate (VO(acac)₂) as catalyst with *tert*-butyl hydroperoxide (TBHP) as oxidant with the aim to identify the most active species for epoxidation and to retrieve insight into the most plausible epoxidation mechanism. The reaction mixture is composed of various inactive and active complexes in which vanadium may either have oxidation state +IV or +V. Inactive species are activated with TBHP to form active complexes. After reaction with cyclohexene each active species transforms back into an inactive complex which may be reactivated again. The reaction mixture is quite complex containing hydroxyl, acetyl acetonate, acetate or a *tert*-butoxide anion as ligands and thus various ligand exchange reactions may occur among active and inactive complexes. Also radical decomposition reaction allow transforming V^{+IV} to V^{+V} species. To obtain insight into the most abundant active complexes, each of previous transformation steps has been modeled through thermodynamic equilibrium steps. To unravel the nature of the most plausible epoxidation mechanism, first principle chemical kinetics calculations have been performed on all proposed epoxidation pathways. Our results allow to conclude that the concerted Sharpless mechanism is the preferred reaction mechanism and that alkylperoxo species V^{+IV}O(L)(OOtBu) and V^{+V}O(L₁)(L₂)(OOtBu) species are most abundant. At the onset of the catalytic cycle vanadium +IV species may play an active role but as the reaction proceeds, reaction mechanisms that involve vanadium +V species are preferred as the acetyl acetonate is readily oxidized. Additionally an experimental IR and kinetic study has been performed to give a qualitative composition of the reaction mixture and to obtain experimental kinetic data for comparison with our theoretical values. The agreement between theory and experiment is satisfactory.

Keywords: catalysis; epoxidation; vanadyl acetylacetonate (VO(acac)₂); *tert*-butyl hydroperoxide (TBHP); cyclohexene; DFT; chemical kinetics; rate constants

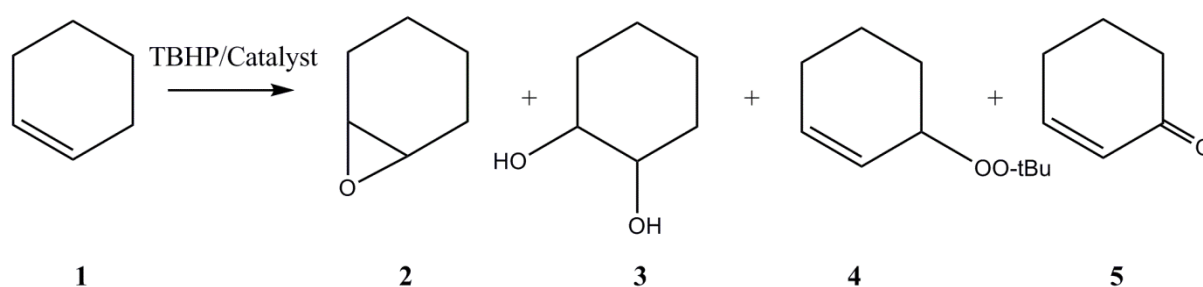
1. Introduction

(Cyclo)alkene epoxidation is a key transformation in organic synthesis both on an academic and industrial scale for the production of various chemicals. Many catalytic systems based on transition-metal complexes of Mo, Ti, W and V have been reported and found to be very effective and selective for the epoxidation of a wide range of (cyclo)alkenes using hydroperoxides as oxidant [1-3]. The reaction chemistry of vanadyl acetylacetonate ($\text{VO}(\text{acac})_2$) as catalyst for the oxidation of cyclohexene with hydrogen peroxide or *tert*-butyl hydroperoxide (TBHP) as oxidant has been the subject of several experimental studies [4-8]. Recently, the homogeneous $\text{VO}(\text{acac})_2/\text{TBHP}$ system and the porous metal organic framework type catalyst MIL-47 [9] have been compared for their cyclohexene epoxidation activity and they showed similar conversion patterns [10, 11]. In view of our interest in both the homogeneous ($\text{VO}(\text{acac})_2$) system and the heterogeneous epoxidation cycles on MIL-47, it is important to obtain mechanistic insight into the plethora of reactions possible for the $\text{VO}(\text{acac})_2/\text{TBHP}$ system. Herein, we have investigated various epoxidation pathways for this catalytic system theoretically. Additionally new kinetic experiments were performed to compare the theoretical kinetic data with the experimentally observed trends. The investigated reaction routes are as complete as possible, taking into account vanadium species in oxidation state +IV and +V, with a variety of ligands and with the additional account of reaction that allow changing the oxidation state. To the best of our knowledge no full mechanistic proposal of all possible reactions has been proposed, but yet there are a series of experimental and theoretical studies providing very relevant information.

The $\text{VO}(\text{acac})_2/\text{TBHP}$ system has already received considerable attention due to a variety of interesting applications. More information can be found in vanadium chemistry reviews [12-15] but some interesting highlights on applications are given hereafter. $\text{VO}(\text{acac})_2$ is readily oxidized to V^{+V} complexes upon treatment with a peroxide and vanadium(V) complexes have been found to act as catalyst precursors in various oxidation reactions such as bromination reactions, epoxidations of alkenes and allylic alcohols, oxidations of sulfides to sulfoxides and sulfones, hydroxylations of alkanes and arenes, and oxidations of primary and secondary alcohols to the corresponding aldehydes and ketones [13, 15]. The $\text{VO}(\text{acac})_2$ -catalyzed epoxidation of allylic alcohols with alkyl hydroperoxides provides a useful route to epoxidize alcohols [4, 15-17]. By using proline-derived hydroxamic acids as chiral ligands, even higher enantioselectivities (up to 80% enantiomeric excess) could be achieved [12, 17]. Furthermore, the $\text{VO}(\text{acac})_2/\text{TBHP}/\text{ligand}$ system allows the highly chemoselective mono-epoxidation of olefinic alcohols like geraniol [18, 19], as unfunctionalized alkenes react more slowly with this system. The active species have been identified in stoichiometric reactions as mononuclear oxoperoxovanadium(V) complexes, of which some have been structurally characterized [20]. The catalyst $\text{VO}(\text{acac})_2$ forms different complexes and experimental studies have been conducted to demonstrate the various transformations $\text{VO}(\text{acac})_2$ undergoes upon treatment with TBHP.

$\text{VO}(\text{acac})_2$ is rapidly converted to vanadate esters ($\text{VO}(\text{OR})_{3-x}(\text{OOR})_x$, with $\text{R}=\textit{tert}$ -butyl and $x \in \{1,2,3\}$) in presence of TBHP, and the oxidation products were found to be also acidic, just as Hacac [7, 21, 22]. Upon treating $\text{VO}(\text{acac})_2$ with an excess of TBHP, typically in the proportion of $\text{VO}(\text{acac})_2:\text{TBHP} > 10$ as in mild oxidation conditions (benzene, 20 °C), acetylacetonate (acac)-ligands are eliminated and oxidized. In all cases these reactions are exothermic. The most abundant oxidation product of Hacac was found to be acetic acid (HOAc) [7, 23]. Furthermore, certain studies have tried to unravel the initial steps in the reaction of $\text{VO}(\text{acac})_2$ with TBHP [7, 8]. The active intermediates were widely accepted to be vanadium(+V) alkylperoxo complexes in the $\text{VO}(\text{acac})_2/\text{TBHP}$ [4, 16, 17, 22] and $\text{VO}(\text{acac})_2/\text{TBHP}/\text{ligand}$ [24-28] catalytic systems. More specifically, Talsi et al. [8] investigated the role of alkylperoxo complexes for the cyclohexene epoxidation with organic hydroperoxides in

presence of $\text{VO}(\text{acac})_2$ in detail by NMR and EPR. Experimentally, V^{+V} alkylperoxo species ($\text{V}^{+V}\text{O}(\text{O}t\text{Bu})$) have been thought to epoxidize cyclohexene [8]. Those alkylperoxo species are also able to oxidize cyclohexene, but only through radical generation via the equilibrium $\text{V}^{+V}\text{O}(\text{OOR}) \leftrightarrow \text{V}^{+IV}\text{O} + \bullet\text{OOR}$. Moreover, when cyclohexene is added to the $\text{VO}(\text{acac})_2/\text{TBHP}$ system, it is converted in various products [10] (see **Scheme 1**). The desired product is usually cyclohexene oxide which consecutively converts into cyclohexane-1,2-diol in presence of water and acid, while *tert*-butyl-2-cyclohexenyl-1-peroxide and 2-cyclohexene-1-one are byproducts formed by radical side reactions and alcohol oxidations. Here, we will exclusively focus on the epoxidation mechanism for unfunctionalized alkenes, so the species active for epoxidation need to be identified.



Scheme 1: Possible reaction products formed during the oxidation of cyclohexene with $\text{VO}(\text{acac})_2$ as a catalyst and TBHP as oxidant.

From a computational point of view, there are to the best of our knowledge no theoretical investigations on the epoxidation reaction with THBP on vanadium species so far. It might be anticipated that similarities will be present with the epoxidation reaction cycle in which hydrogen peroxide is used, but still some differences might occur due to the more bulky TBHP molecule. Apart from this, some interesting computational studies on the vanadium-catalyzed olefin epoxidation are available, which all use hydrogen peroxide H_2O_2 as oxidant [29-32]. We particularly mention the work of Kuznetsov et al. [31] where different pathways of the reaction of divanadium-substituted polyoxotungstate with hydrogen peroxide and olefin were studied using DFT methods and where the role of solvent is also taken into account with explicit water molecules or a polarizable continuum model with acetonitrile as solvent.

Another recent theoretical study concerns the epoxidation of olefins catalysed by vanadium-salan complexes [32]. Therein, three main routes were investigated, i.e. the Mimoun, the Sharpless and the biradical mechanisms. In that case it was found that the epoxidation of the VO-salan complexes preferably happens via a concerted Sharpless route [33]. Bühl et al. [29] came to the same conclusion in their study on $[\text{VO}(\text{O}_2)_2(\text{Im})]^-$ species solvated in water, where also the effect of various substituents was tested in relation with the barrier for epoxidation and ^{51}V -NMR shift. In another recent study, Kirilova et al. [34] presented a kinetic scheme for oxidations in the vanadate/pyrazine-2-carboxylic acid (PCA) system. The mechanism of radical generation was studied, as these catalytic systems activate C–H bonds via such radical pathways. The generation of both $\bullet\text{OH}$ and $\bullet\text{OOH}$ radicals was modeled via thermodynamic equilibrium steps of various catalytic cycles containing both +IV and +V species. Side reactions such as keton formation from an alcohol, have been modeled in detail by Sauer and coworkers on vanadium surfaces [35-38]. During this reaction, the oxidation state of the vanadium goes from +V to +III. Therefore the broken symmetry approach has been applied for the description of the transition state for the keton formation [35].

Molecular modeling of the homogeneous epoxidation of cyclohexene with $\text{VO}(\text{acac})_2/\text{TBHP}$ is very complex due to the presence of multiple complexes that can be formed [8, 21]. The cyclohexene conversion also changes with reaction time, as more and more byproducts are formed such as *tert*-butanol (tBuOH) and *tert*-butyl-2-cyclohexenyl-1-peroxide **4**, inhibiting further conversion [8]. In addition, this distribution can be affected by solvents, pH, addition of ligands, usage of radical catching species, etc.

The aim of this study is twofold: (1) identifying the most abundant, active epoxidation complexes and (2) investigating the probability of various proposed reaction mechanisms and eventually establish the most plausible one. To achieve this goal, a whole family of active and inactive complexes which can either have oxidation state +IV or +V for vanadium have been considered, where also the ligand has been varied. The transformation among the different species has been modeled as thermodynamic equilibrium steps. After that first principle chemical kinetic data have been calculated for each of the active species and for each of the proposed mechanistic cycles in literature. To cross validate our theoretical data with experiments, also new experimental kinetic data have been produced. As such this study should allow to provide a nearly complete picture of the epoxidation of cyclohexene through the homogeneous catalytic $\text{VO}(\text{acac})_2/\text{TBHP}$ system.

2. Overview of epoxidation mechanisms and various active and inactive complexes

2.1 Active versus inactive complexes

Before starting the actual epoxidation reaction, the $\text{VO}(\text{acac})_2$ needs to be brought into an active complex (AC) after reaction with the oxidant TBHP. There are various possibilities for the generation of active species, which will be outlined below. The whole catalytic cycle consists in principle of two main reaction families: the epoxidation of cyclohexene bringing the catalyst into an inactive complex (IC), and the activation of inactive to active complexes through reaction with the oxidant TBHP. Apart from these reaction families, radical decomposition reactions allow altering the oxidation state from +IV to +V or vice versa. These main categories are schematically shown in **Figure 1**.

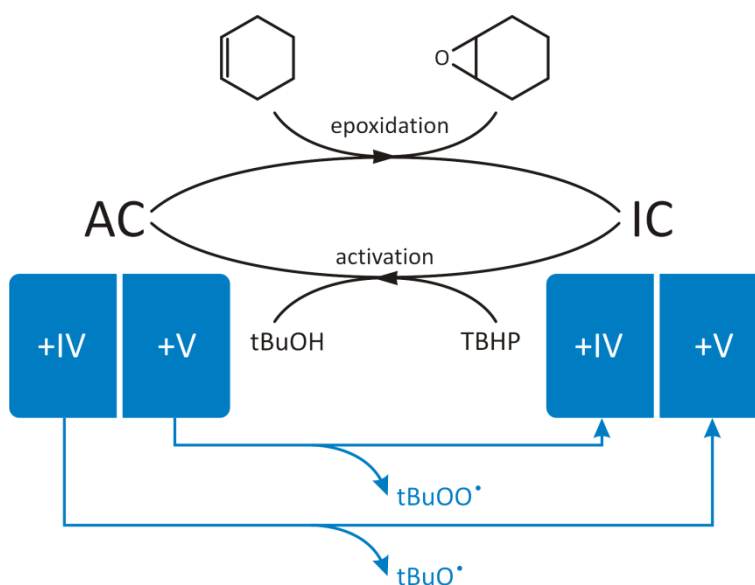


Figure 1: Main reaction families of the VO(acac)₂/TBHP catalytic system for epoxidation of cyclohexene, transforming active complexes (AC) to inactive complexes (IC). The scheme reports *tert*-butanol as most dominant side-product of the activation step. Side reactions where radicals (tBuOO•, tBuO•) are generated, start as well from active complexes

Initial Activation of VO(acac)₂: One possibility for generating active complexes was suggested by Stepovik [7] and is illustrated in **Figure 2**. In this picture VO(acac)₂ **6** loses one of its acetylacetonate ligands with formation of Hacac **9**, that may further oxidize to acetic acid (HOAc) [7, 23]. This reaction is irreversible due to the strong exothermic nature of the reaction (reaction energy of -1172 kJ/mol at 0K) and the escape of the CO₂. As such Hacac will become less abundant as the catalytic cycle of epoxidation evolves and is responsible for the abundant presence of acetic acid in the reaction mixture. HOAc may then play a significant role in the further catalytic system through ligand exchange reactions, as will be explained further in this paper. Apart from this activation step which occurs initially, a variety of other activation steps have been considered in this paper which will be discussed further in this section.

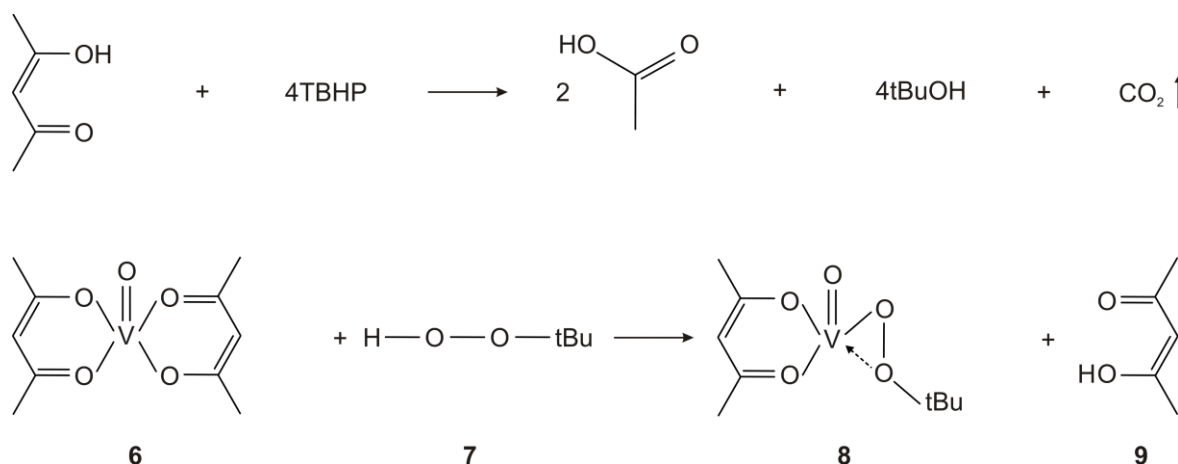


Figure 2: Ligand exchange in the initial stage of the catalytic cycle forming an active complex **8**.

Radical decomposition of active complexes: The vanadium +IV alkylperoxo complex **8** of **Figure 2** is one possible active complex but in the early stages of the epoxidation reaction with an excess of TBHP in the reagent mixture, various radical decomposition pathways may also occur. Some examples of such pathways are shown in **Figure 3**, although these are only illustrative examples and are far from unique. They allow transforming V^{+IV} → V^{+V}, giving rise to the alkylperoxo species of the type VO(acac)₂OOR (R=H or tBu), which were observed in the experimental work of Talsi et al. [8]. This has been confirmed by a more recent experimental work [8]. However, in the absence of spin traps (in benzene at 20 °C) the EPR spectrum measured just after mixing of reagents shows a signal which could be assigned to the coordinated VO(acac)₂ – TBHP complex with vanadium in oxidation state +IV. Hence, this work gives evidence that both +IV and +V vanadium alkylperoxo complexes are present during the reaction of VO(acac)₂ with TBHP. An excess of TBHP in the reagent mixture also lead to the complete disappearance of the V^{+IV} signal in the EPR spectrum. These observations point towards the existence of radical decomposition mechanisms. The examples given in **Figure 3a**

concern a homolytic cleavage of the peroxy linkage of the alkylperoxocomplex **10** with formation of a tBuO• radical and a dioxo-complex **11**. The equilibrium displayed in **Figure 3b** suggests a correlation between the concentration of the active VO(L₁)(L₂)(OOtBu) complex and that of tBuOO• as most stable free radical in solution, which is indeed observed in the work of Talsi [8].

Previous examples given in **Figures 3a** and **3b** are non restrictive and both V^{+IV} and V^{+V} monoperoxo complexes can be formed by various reaction mechanisms for example by ligand exchange. The most straightforward choice for the ligand L represents an acetyl acetonate (acac) ligand, but the concept may easily be generalized with other ligands such as hydroxyl, acetate or a *tert*-butoxide anion which are schematically represented in **Figure 3c**. Indeed from the NMR spectra reported in the work of Talsi [8], evidence was given for other vanadium +V complexes, for instance species with one or more hydroxyl groups as ligands. Ligand exchange reactions lie on the origin of the formation of other active complexes with various ligands. A more general representation of all considered active and inactive complexes in this work is given in **Figure 4** and will be discussed further below. The proposed reactions and equilibrium steps for changing the oxidation state are completely equivalent with similar work done by Kirilova et al. [34].

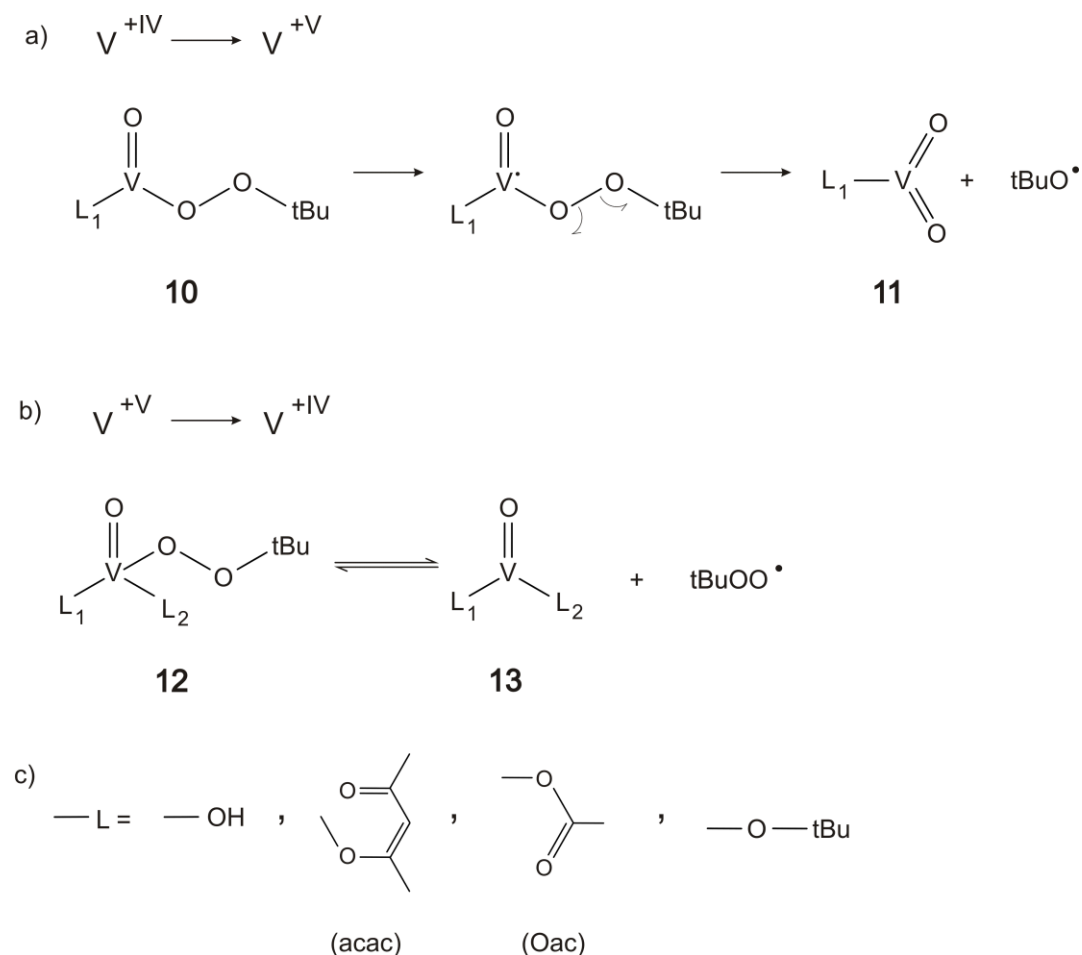


Figure 3: Example of possible radical decomposition reactions: a) oxidation of V^{+IV} in an alkylperoxocomplex induced by homolytic cleavage of the peroxy-linkage; b) formation of the peroxy radical and an inactive V^{+IV} complex; c) ligand choices throughout this paper.

Activation Reactions: After epoxidation, the active complexes (AC) turn back into inactive complexes (IC) and in order to react with cyclohexene they need to be reactivated. This activation step occurs *in situ* by activation reactions with the help of the peroxides HOOR after which active complexes (AC) are formed again, as schematically shown in **Figure 1**. The most relevant structures for inactive and active complexes are given in **Figure 4**. The transformation from active to inactive and vice versa is described as thermodynamic equilibrium steps. Generic structures for the various types of inactive complexes (IC) are represented by the compounds **13** and **15** for V^{+IV} and **11** and **18** for V^{+V} in **Figure 4**. Active vanadium peroxy compounds may be formed by coordination with the alkylhydroperoxide (complexes **14** and **17**), by ligand exchange reactions with the alkylhydroperoxide (complexes **10**, **16**, **19** and **12**) and as the result of TBHP addition to a V=O bond (complexes **12(L₂=OH)** and **20**) (see **Figure 4**).

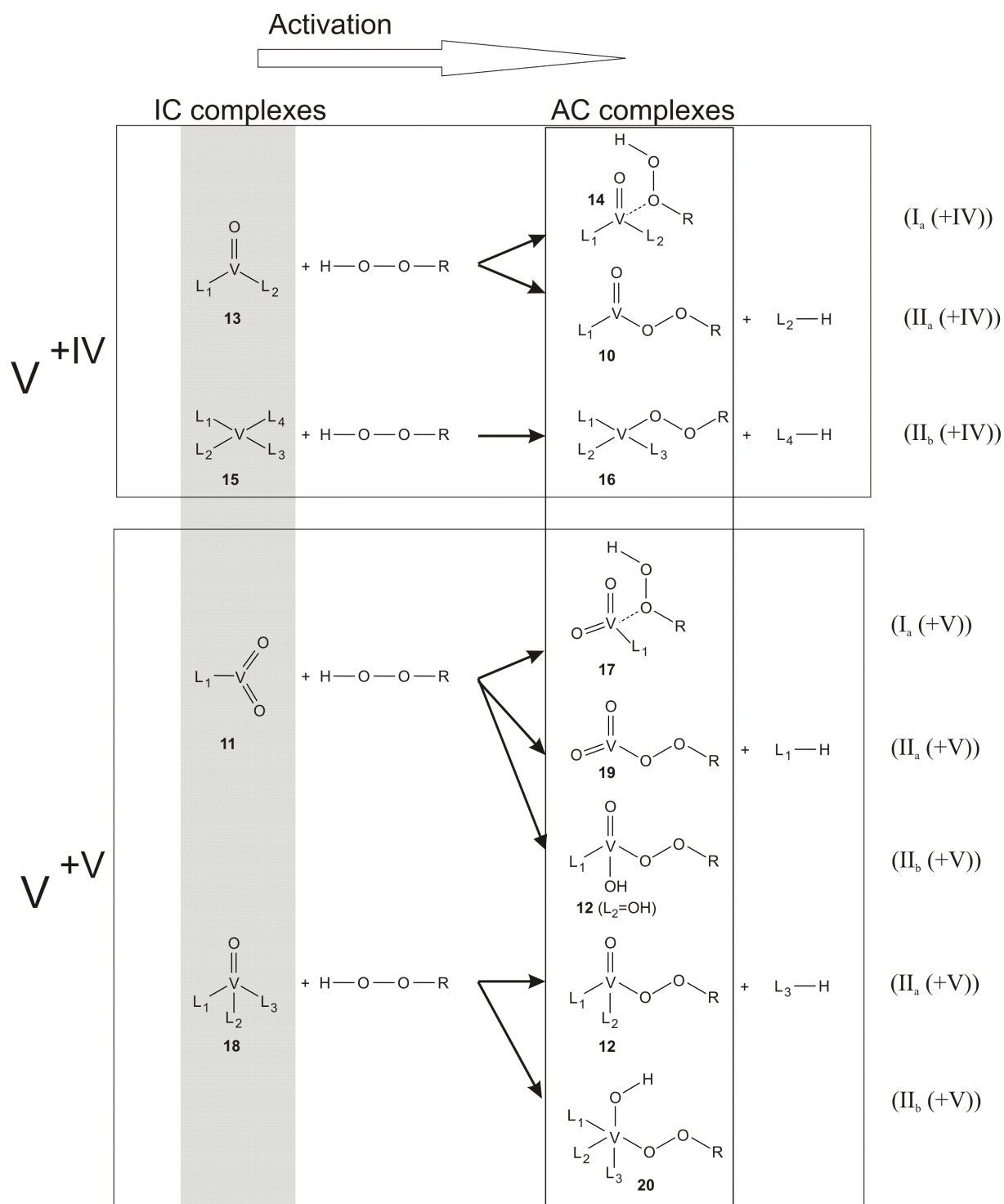


Figure 4: Generic structures for the inactive complexes are given in the grey shaded region. Activation steps to the formation of active complexes take place after reaction with TBHP. Once the active complexes are formed they may undergo epoxidation along various mechanistic cycles which are indicated with Roman indices in the figure. The different classes **Ia**, **Ib**, **IIa**, **IIb** and **III** of reaction mechanisms are defined in **Figure 6**.

Gibbs free energy surfaces for inactive (IC) and active complexes (AC): As already mentioned, all inactive (IC) and active complexes (AC) are linked with each other through equilibrium steps. A

generic scheme is shown in **Figure 5**. Most of them are generated by ligand exchange reactions. The monoperoxo species **21** are not formed by simple exchange reactions, but further details on their formation will be given in **Section 5.3**.

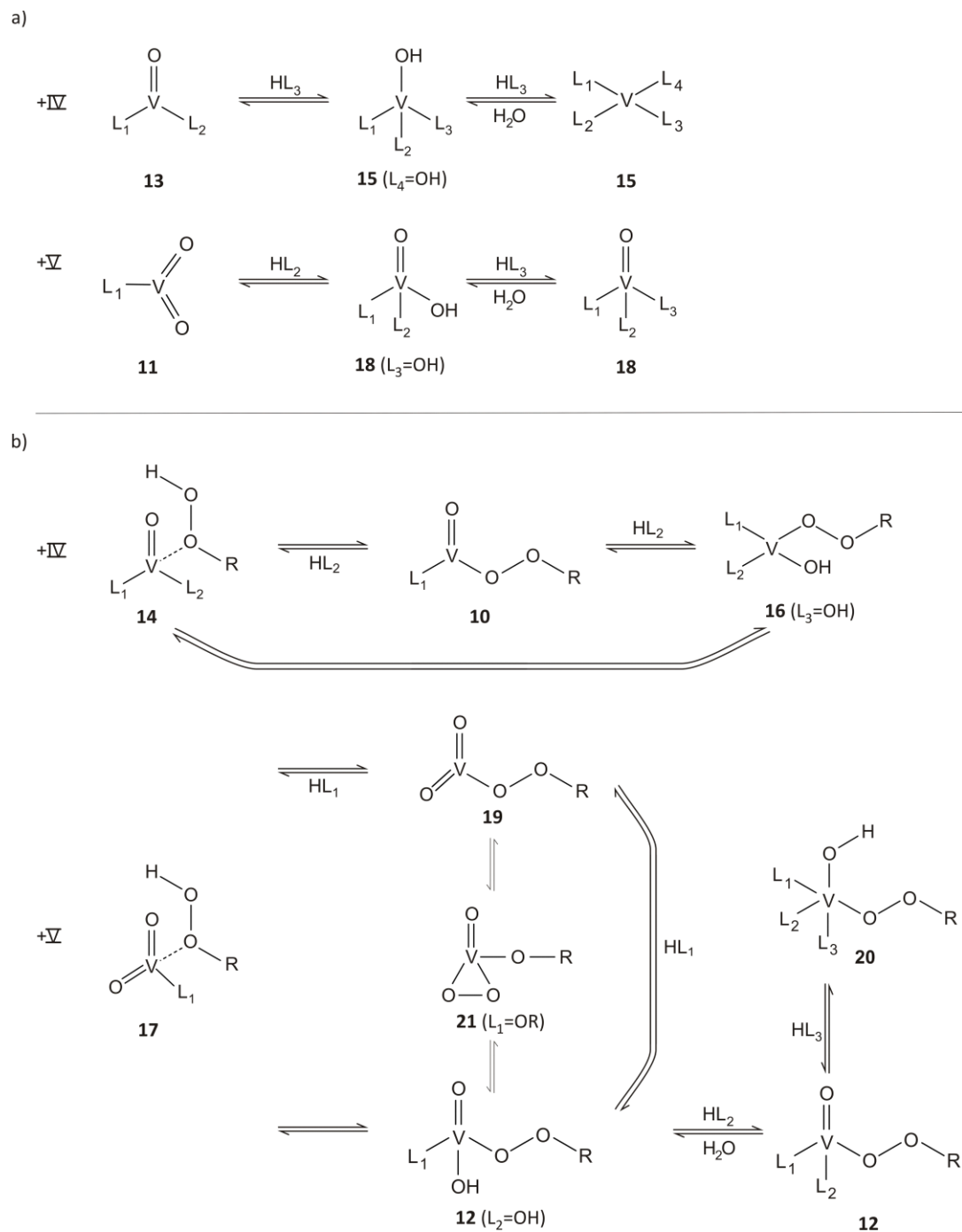


Figure 5: a) Equilibrium steps between different inactive complexes (IC); b) Equilibrium steps between various active complexes (AC).

2.2 Epoxidation mechanism:

Once the active complexes are formed, epoxidation of cyclohexene may take place. Hereafter, we give an overview of all possible epoxidation mechanisms of mono-vanadium complexes with peroxides H_2O_2 or TBHP as oxidant (represented by the notation ROOH with $\text{R} = \text{H}$ or tBu), which were already suggested in literature. All mechanistic proposals start from active mono-vanadium complexes which have either oxidation number +IV or +V. They are schematically represented in **Figure 6**. Three reaction classes are distinguished, which are labeled by roman numbers **I**, **II** and **III** and which are viable both for vanadium in oxidation state +IV and +V. For each of the reaction families a schematic representation of the transition state is also given.

Within reaction family **I** the peroxide is coordinated with the metal. This mechanism was already proposed in the early seventies [4, 39-43]. In mechanism **Ia** the electron-deficient oxygen of the hydroperoxide ROOH is placed in the vicinity of the double bond in the transition state. As such the epoxidation reaction is favored over the decomposition of the hydroperoxide. A hydrogen transfer occurs from the coordinated peroxide to the oxo-ligand in the vanadium complex. Mechanism **Ib** differs only slightly from **Ia**. In this case the peroxide hydrogen undergoes a transfer to a ligand (L_2 in **Figure 6**) with the cleavage of the metal-ligand bond. It might be anticipated that reaction families **Ia** and **Ib**, would not be preferred in case TBHP is used as oxidant due to the bulkiness of this species and the steric hindrance with the various ligands. It was already reported earlier that those mechanisms fail to explain the exceptional epoxidation reactivity of allylic alcohols [4, 16, 42]. Although the validity of this reaction class will be investigated by modeling for each of the involved species thermodynamic and kinetic data.

In the second class **II** the intermediate is a monoperoxo complex where the (cyclo)alkene attacks the peroxy-ligand. It is a concerted one-step process and is called a Sharpless-type mechanism [16, 33, 44]. This mechanism enables to explain the exceptional epoxidation reactivity observed for allylic alcohols. The direction of approach is now ideal for an allylic alcohol, which is simultaneously coordinated through its hydroxyl group to the vanadium center (see **Ila** and **Ilb** in **Figure 6**).

The third class of epoxidation reactions **III** starts from peroxy species **21** as active oxidant. There are many mechanisms possible to form this high energetic species from reaction of TBHP with the oxometal group of the catalyst. Plausible routes have been proposed by Chong and Sharpless [44], and some of them will be discussed later in the paper. The occurrence of peroxy complexes of the type **21** with vanadium in oxidation number +IV is less probable, as these complexes require an excess of the peroxide and under these circumstances we may expect oxidation of V^{+IV} to V^{+V} .

Apart from the three mechanisms, there also exists another mechanism – the so-called Mimoun-type mechanism [45] – in which the (cyclo)alkene first coordinates with the metal before reacting with the peroxide, followed by the formation of a five-membered cyclic intermediate which decomposes to epoxide and catalyst. The Mimoun-type mechanism has been intensively studied by **Kuznetsov and Pessoa** [32] in the olefin epoxidation catalysed by a vanadium-salan complex. However, they found no stable π -complexes for the coordination of the double bond of the alkene with the metal, and this is probably due to the high oxidation state of the transition metal. In addition the activation barrier to form a five-membered metallocyclic intermediate turns out to be too high. They conclude that the Mimoun-type mechanism may be ruled out. Therefore, the Mimoun mechanism will not be further examined in this work and focus will be made on the Sharpless-type mechanism.

The mechanisms taken up in **Figure 6** are meant to give a global overview of various mechanistic proposals for epoxidation starting from a mixture of active complexes. Those complexes that are not figuring in the scheme are either energetically too activated or show a structure with too many ligands hindering any flexibility for further reaction. In addition almost all active complexes are linked through reaction equilibriums – they will be discussed later – and in this respect structures which are not taken up in the scheme can in most cases be brought back to one of the classes sketched in **Figure 6**.

In view of all these considerations it is obvious that the total number of possible active complexes (AC) may be very high. This is especially true when taking into account all possible ligand combinations that can be formed. Realistic choices for ligands in this epoxidation study with $\text{VO}(\text{acac})_2$ are given in **Figure 2c**. Each AC generates its own reaction kinetics. To prevent unnecessary transition state computations for reactions that are unlikely to occur, we exclude the possibility that the acetyl acetonate and acetate ligand appears twice in the same monovanadium complex. Also experimentally it was shown that $\text{VO}(\text{acac})_2(\text{OOR})$ could not be responsible for the catalytic activity in epoxidation of cyclohexene [8].

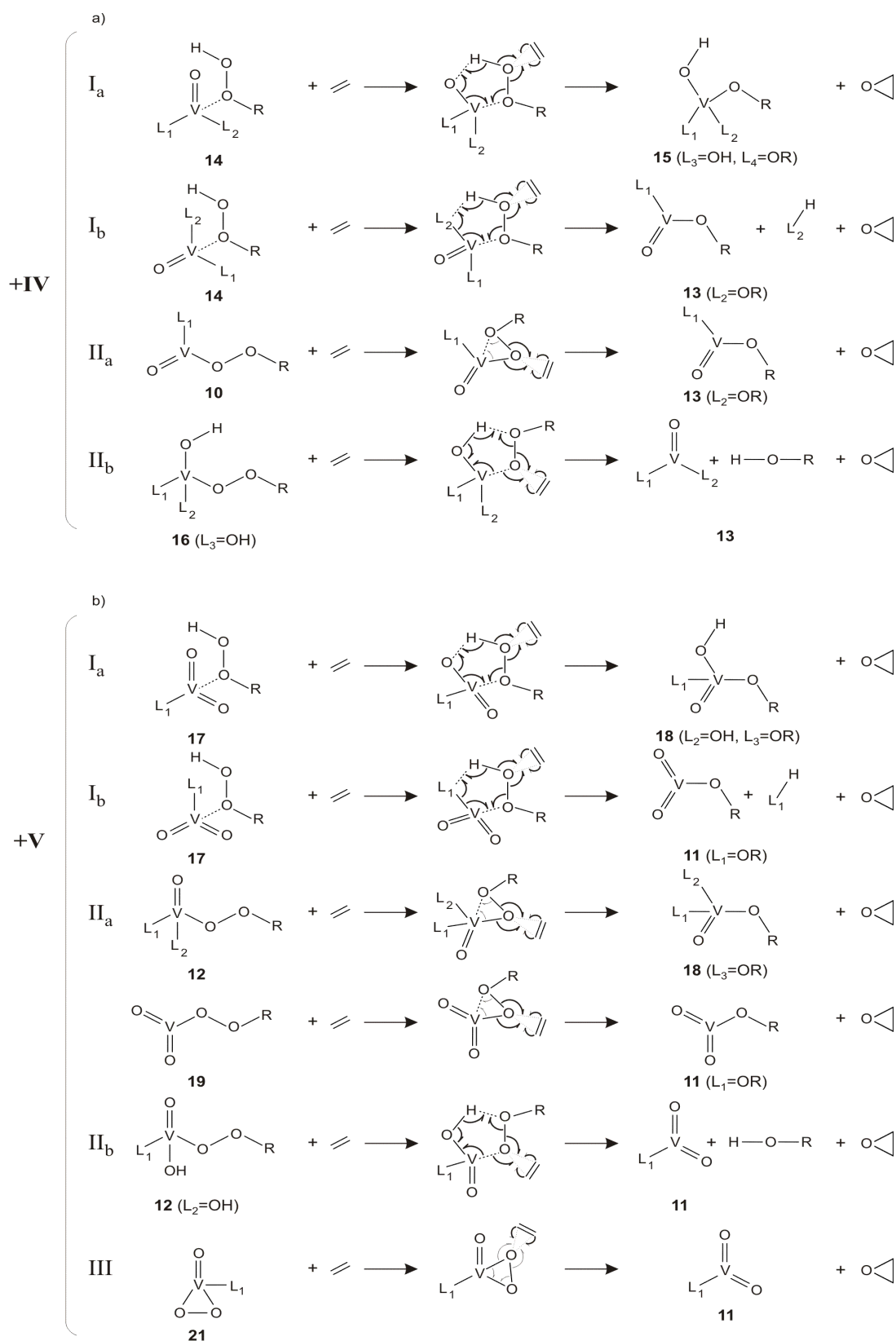


Figure 6: Various reaction mechanisms for the epoxidation reaction. Both vanadium species in oxidation state +IV and +V are taken up.

3 Computational methods

The proposed catalytic cycles for the homogenous epoxidation of cyclohexene ($\text{VO}(\text{acac})_2 + \text{TBHP}$) were studied theoretically by means of Density Functional Theory (DFT). All intermediates and transition states were fully optimized at the DFT level of theory using the B3LYP hybrid functional [46, 47] and usage of the Gaussian03 package [48]. The double-zeta Pople basis set 6-31+G(d) was used for all the atoms except for vanadium, for which the LANL2DZ effective core potential and basis set was applied [49]. The frequencies were calculated at the same level of theory as the geometry optimizations and confirmed that all structures were either local minima on the potential energy surface or transition states. Afterwards the energies were refined by single point energy calculations at the B3LYP/6-311+g(3df,2p) level of theory. This type of procedure is commonly used in theoretical calculations on transition metal catalysis [34, 50, 51]. Furthermore, also the van der Waals corrections as developed by Grimme were included [52]. More specifically, the dispersion corrections are calculated according to the third version of Grimme [53] by using the ORCA program [54]. Using standard notation "LOT-E"/"LOT-G" (LOT-E and LOT-G being the electronic levels of theory used for the energy and geometry optimizations, respectively), all results discussed in this paper are obtained with the method denoted as "B3LYP/6-311+g(3df,2p)-D3// V: B3LYP/LANL2DZ + LANL2DZ-ecp; O, C, H: B3LYP/6-31+g(d)".

In this paper, both the unimolecular and bimolecular rate coefficients will be determined for the epoxidation reaction. Both approaches differ by the reference level that is used for the reactants [55]. A schematic energy diagram for the epoxidation reaction of cyclohexene is given in Figure 6. In case of the intrinsic approach, one starts from the reactant level where the various reacting species are fully adsorbed at the active complex (referred as pre-reactive complex in **Figure 7**). In case of the bimolecular approach, the reactant level is taken as the active vanadium complex (AC) with cyclohexene in the gasphase.

All considered reactions are strongly exothermic, which is reflected in a high backward reaction barrier (in most cases even higher than 200 kJ/mol). Therefore only the forward reaction will be considered in the main paper (backward reaction parameters can be found in supporting information). In order to find the correct pre-reactive complex, IRC calculations were performed starting from the transition states. All reaction rate constants are obtained using classical transition state theory. Within the unimolecular approach this gives following expression for the rate coefficient k_{uni} (s^{-1}):

$$k_{fwd,uni}(T) = \frac{q_{TS}(T)}{q_R(T)} \exp\left(-\frac{\Delta E_{0,int}^\ddagger}{RT}\right), \quad (2)$$

with $\Delta E_{0,int}^\ddagger$ the intrinsic reaction barrier at 0 K (**Figure 7**).

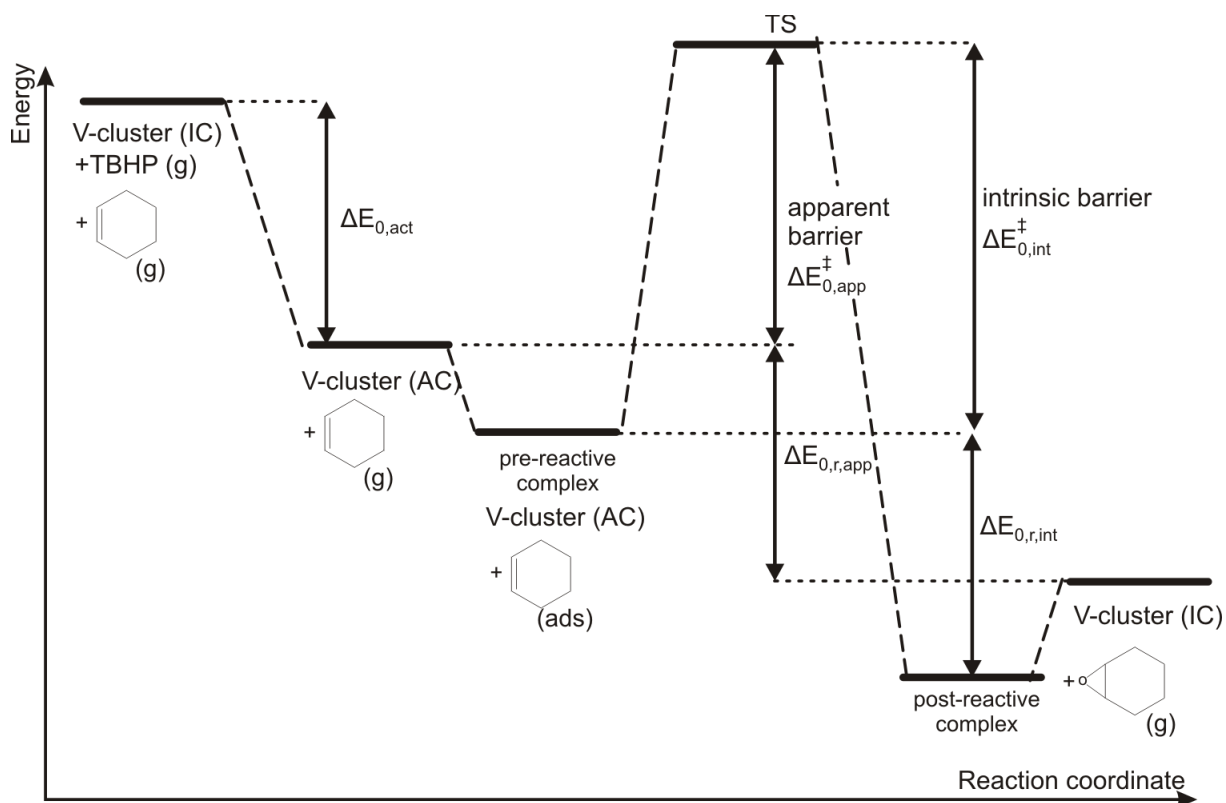


Figure 7: Schematical energy diagram for the epoxidation reaction of cyclohexene and an active mono-vanadium peroxo complex. For an unimolecular approach relevant energies are the intrinsic barrier $\Delta E_{0,int}^\ddagger$ and reaction energy $\Delta E_{0,r,int}$ referred to the fully physisorbed pre-reactive or post-reactive complex. For a bimolecular description, the apparent energy barriers $\Delta E_{0,app}^\ddagger$ and apparent reaction energies $\Delta E_{0,r,app}$ are used. $\Delta E_{0,act}$ is the energy difference between the inactive complex and the activated complex.

Within the bimolecular approach, the reactants consist of cyclohexene (CH) and an activated complex (AC) and the rate constant $k_{fwd,bi}$ ($\text{m}^3 \text{mol}^{-1} \text{s}^{-1}$), is given by the following expression :

$$k_{fwd,bi}(T) = \frac{q_{TS}(T)}{q_{AC}(T) q_{CH}(T)} V \exp\left(-\frac{\Delta E_{0,app}^\ddagger}{RT}\right) \quad (3)$$

with $\Delta E_{0,app}^\ddagger$ the apparent reaction barrier at 0 K (**Figure 7**).

All other reactions in the catalytic cycle apart from the epoxidation reaction are described as equilibrium steps. Fast equilibrium processes exist between the various species belonging to the family of inactive (**Figure 5a**) and active complexes (**Figure 5b**) which in turn are subdivided into vanadium +IV or vanadium +V classes. A third class of equilibrium processes concerns the activation reactions (**Figure 4**) connecting the family of inactive to the family of the active species. In all equilibrium steps the oxidation state of the vanadium is kept fixed (+IV or +V), and transition between vanadium complexes with different oxidation number only takes place via radical decomposition reactions as outlined in **Figure 3**. Most of the equilibrium reactions represent ligand exchange reactions. In this last category, the equilibrium coefficient is calculated as follows:

$$K_P(T) = \frac{q_B(T) \cdot q_{HL2}(T)}{q_A(T) \cdot q_{HL1}(T)} \cdot \exp\left(-\frac{\Delta E_{0,r}}{RT}\right) = \exp\left(-\frac{\Delta G_{323,r}}{RT}\right), \quad (4)$$

for the reaction schematically written by complex A + HL₁ ⇌ complex B + HL₂.

Herein, $\Delta E_{0,r}$ and $\Delta G_{323,r}$ represent respectively the reaction energy at 0 K and the Gibbs free energy at 323 K.

The calculation procedures for all rate coefficients k and K are now implemented in an in-house developed software module TAMKIN [56].

4 Experimental characterization and kinetics for epoxidation of cyclohexene

This experimental section contains an infrared (IR) and gas chromatography (GC) study carried out to characterize various species present in the reaction mixture. The results on the UV-Vis and GC are taken up in the SI. Additionally, experimental kinetic parameters for the epoxidation of cyclohexene have been determined which can then directly be compared with the theoretically determined rates.

4.1 IR

The IR measurements were recorded on a Bruker EQUINOX 55 FTIR spectrometer. The liquid samples were measured between KBr plates at room temperature. An accumulation of 100 scans was done of each sample. Three samples with increasing V/TBHP ratio were prepared in a mixture of 0.0055 mol catalyst with *tert*-butyl hydroperoxide (TBHP) solved in decane. Their specific composition is tabulated in **Table 1**. The samples are presented with increasing amount of oxidant.

Table 1: Composition of the liquid samples.

	ratio V/TBHP	TBHP (mol)	VO(acac) ₂ (mol)	chloroform (mL)
Sample 1	2	0.00275	0.0055	10
Sample 2	2/1.5	0.00412	0.0055	10
Sample 3	0.5	0.0110	0.0055	10

Figure 8 presents the liquid phase infrared spectra of the mixtures described in Table 1, measured within a few minutes after mixing the ingredients at room temperature. It is not surprising that these infrared spectra are very rich, as they contain a mixture of several infrared active species. As a consequence, the vibrations that are typical for acetylacetonate ligands (1562 cm⁻¹ for the C=O and 1526 cm⁻¹ for the conjugated C=C stretch) [57] are overwhelmed by other vibrations, e.g. the CH₂ deformation of decane (solvent of TBHP) and CH₃-C deformation of TBHP, both located around 1500 cm⁻¹. However, there is a clear window around 1700 cm⁻¹ and the C=O stretch vibration that is very typical of the acetate can be nicely seen at 1715 cm⁻¹ [58]. The peak intensity of the acetate clearly increases by raising the amount of TBHP. So, if more oxidant is added, then more acetylacetonate ligands oxidize towards acetate esters and acetic acid. This is a nice experimental validation of the proposal of Stepovik [7] to initially generate active complexes (**Figure 1**).

In order to strengthen the experimental validation, we repeated the experiment with two different solvents: toluene and acetonitrile. The results are reported in the SI, but confirm the experiment with decane as solvent.

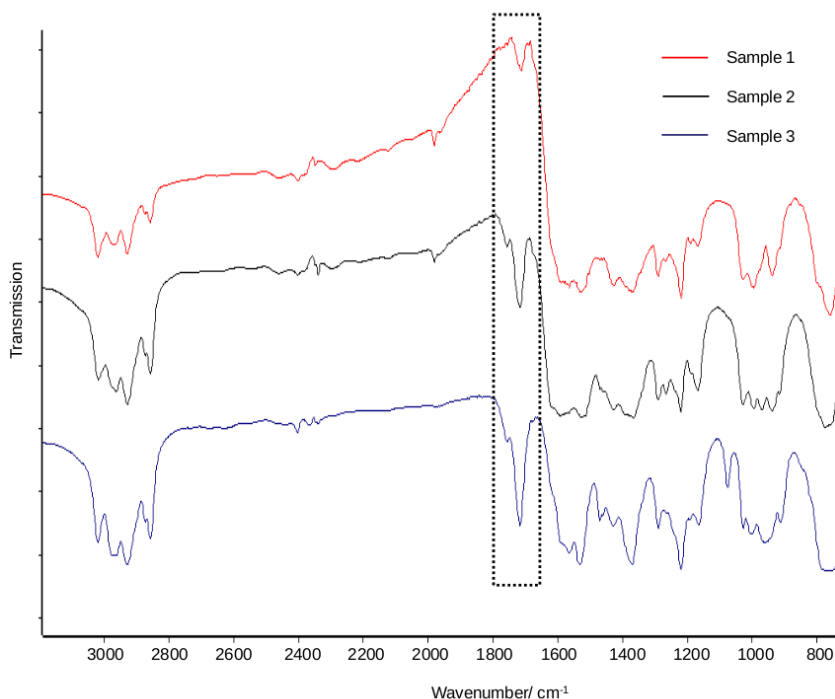


Figure 8: IR spectra of samples 1 to 3 with the composition described in **Table 1**.

4.2 Kinetic study

An experimental setup has been established to determine kinetic parameters for the epoxidation of cyclohexene. Therefore, experiments have been performed at different temperatures, with varying cyclohexene and *tert*-butyl hydroperoxide concentration, working in diluted conditions (solvent: chloroform). For extended details, e.g. experimental setup and different initial concentrations we refer to the Supporting Information.

The cyclohexene epoxidation rate R is assumed to be first order in the cyclohexene concentration $[CH]$ and the concentration of all active vanadium species $[V^{AC}]$:

$$R = \frac{d[CH-ox]}{dt} = k \cdot [CH] \cdot [V^{AC}] \quad (5)$$

with k , the rate coefficient for the epoxidation reaction of cyclohexene ($\text{m}^3 \text{mol}^{-1} \text{s}^{-1}$) towards cyclohexene oxide **2**. An equilibrium is further assumed between the active vanadium (V^{AC}) and the inactive vanadium (V^{IC}) species (This will be extensively discussed in the theoretical results section). Activation of the inactive complexes takes place after reaction with TBHP :



The corresponding equilibrium coefficient K_{act} (m^3/mol) for this activation reaction is easily calculated as:

$$K_{act} = \frac{[V^{AC}]}{[V^{IC}] \cdot [TBHP]} \quad (6)$$

Assuming a constant total concentration of vanadium $[V^0] = [V^{IC}] + [V^{AC}]$, which is determined by the initial vanadium concentration, a straightforward calculation leads to an expression of the cyclohexene epoxidation rate R in terms of the concentration of the vanadium catalyst, cyclohexene and the peroxide :

$$R = \frac{k \cdot [CH] \cdot K_{act} \cdot [V^0] \cdot [TBHP]}{1 + K_{act} \cdot [TBHP]} \quad (7)$$

in agreement what has been reported by Gould et al. [4].

The initial rate R_0 is obtained after considering the initial concentration of cyclohexene $[CH]_0$ in the reaction mixture.

Eq.(7) is rewritten as

$$Y = k \cdot [V^0] \cdot K_{act} - K_{act} \cdot X \quad (8)$$

$$\text{with } Y = \frac{R_0}{[TBHP] \cdot [CH]_0} \text{ and } X = \frac{R_0}{[CH]_0}$$

A plot Y versus X represents a Hofstee-type plot. The intersect with the Y -axis, obtained after extrapolation of the rate data, yields the value of the rate constant k . The absolute value of the slope represents the equilibrium constant K_{act} . Measurements have been done at different temperatures and results are summarized in **Table 2**. For each temperature different runs have been performed with different concentrations of cyclohexene $[CH]_0$ and TBHP $[TBHP]_0$. The Hofstee plots at the various temperatures are given in **Figure S.3** of the Supporting Information. The rate constants k derived from the Hofstee plots for the four temperatures are used as input for an Arrhenius plot of $\ln(k)$ versus $1/T$. It closely approaches a straight line (**Figure 9**) indicating that the extrapolation procedure used to obtain the rates k is free from large random errors. The Arrhenius plot predicts an average pre-exponential factor A of $2.36E+07 \text{ m}^3 \text{ mol}^{-1} \text{ s}^{-1}$ and an activation energy E_a of 48.6 kJ/mol . These kinetic parameters should be regarded as average parameters of all possible active vanadium species, leading to epoxidation of cyclohexene. The values in **Table 2** are in close agreement with those of the paper of Gould et al. [4], also taking in mind that we have been working at other reaction conditions (solvent, different concentrations of cyclohexene, vanadium and TBHP; supporting information for details). Moreover, we could also extract more information from the experiment. The standard enthalpy of activation at 323 K is found to be 43.2 kJ/mol (for a bimolecular reaction $\Delta H_{323}^\ddagger = E_a - 2RT$). The entropic contribution ΔS_{323}^\ddagger amounts to -90.8 J/mol/K , yielding a Gibbs free energy difference ΔG_{323}^\ddagger for the epoxidation reaction of 72.6 kJ/mol . These are interesting values to be compared with the theoretical predictions (see Section 5.6).

The kinetic data obtained here will be validated with the epoxidation mechanisms that are found to be most probable from our theoretical calculations.

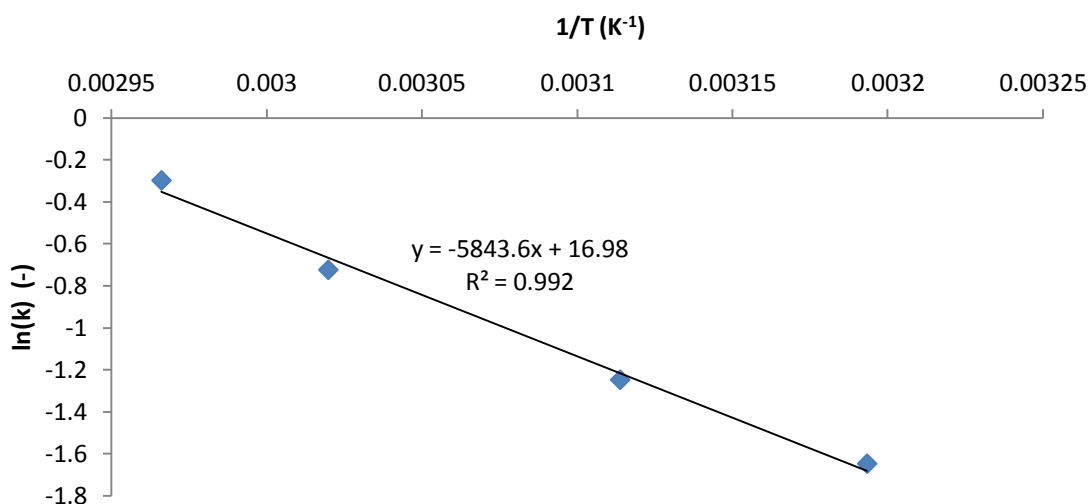


Figure 9: Arrhenius plot: $\ln(k)$ versus $1/T$

Table 2: Overview of the rate constant and equilibrium constant K_p between active and inactive vanadium complexes at different temperatures. (*) experimental value from [4]

	337 K	331 K	321 K	313 K	323 K
k (m ³ /mol/s)	7.4E-04	4.9E-04	2.9E-04	1.9E-04	2.13E-04*
K_{act} (m ³ /mol)	3.18E-03	4.90E-03	8.56E-03	1.79E-02	1.03E-02*

5 Results and discussion on the theoretical calculations

The complete catalytic cycle, including activation, epoxidation and change in oxidation state through radical decomposition reactions is now studied theoretically for all active complexes and ligands as introduced in section 2. This section is structured as follows: first the thermodynamic equilibria between various active complexes are discussed, followed by a similar discussion on the inactive complexes. Then the activation steps allowing the transformation of inactive to active complexes are modeled through thermodynamic equilibrium steps. First principle chemical kinetics are studied for all proposed epoxidation pathways (**Figure 6**) in section 5.4. In section 5.5 we also discuss the radical decomposition pathways that allow to change the oxidation state. At the end of this section our kinetic data on the most abundant species and most probable epoxidation mechanisms are compared with available experimental data from literature and the experimental data from this work.

5.1 Equilibrium between active complexes (AC)

The different equilibria occurring among the active complexes are schematically displayed in **Figure 5b**. For the vanadium +IV complexes, three different types of active complexes are considered corresponding to species **10**, **14** and **16**(L₃=OH), which were already introduced in **Figure 4**. They may

transform into each other through ligand interchanges and by proton hops. With the introduction of four ligands (OH, acac, OAc and OtBu as introduced in **Figure 3c**) the number of different complexes may become very high. To keep this number within reasonable limits, we restricted the calculation of equilibrium steps among active complexes bearing only one acac or OAc ligand per complex, which is a reasonable assumption taking into account the bulkiness of the TBHP as oxidant. The choice of the four ligands is evident, since acetic acid (HOAc) is formed during the oxidation of acetyl acetate (Hacac), as already mentioned in section 2, which was also confirmed by the experimental IR measurement. In addition, the acetate ligand (OAc) prefers a bidentate ligand coordination with vanadium in most of the complexes.

The equilibrium constants for each of these steps were calculated according to the procedure outlined in the computational section. The results for the equilibrium constants and the associated free energies are schematically shown in **Figure 10a**. The complex VO(acac)(OOtBu) **10** is taken as a reference for the free energies for all species bearing vanadium in oxidation state +IV. Vertical moves in the scheme correspond to complexes of the same type VO(L₁)(OOtBu) but with ligand exchange. The other complexes **14** and **16**(L₃=OH) contain an additional ligand L₂. In the scheme of **Figure 10a** only those complexes are retained which are energetically closest to VO(acac)(OOtBu) complex. The latter is the most favored active V^{+IV} compound resulting from the calculations. The notation used for the identification of the other complexes is straightforward: V(OH)(OH)(acac)(OOtBu) stands for active compound **16** with two OH ligands and an acetyl acetate ligand.

Similarly for vanadium +V complexes a selection of equilibrium steps is given in **Figure 10b**. The selection is made on basis of the same criterion as for the vanadium +IV complexes. In this case complex VO(acac)(OH)(OOtBu) belonging to compound family **12** is taken as the reference, although it does not correspond to the most stable complex. From that starting point, all combinations L₁ and L₂ are considered according to the imposed restrictions on the ligand choices. By subsequent ligand exchange reactions all active V^{+V} complexes taken up in **Figure 5b** are reached. On basis of the Gibbs free energy profiles (at 323 K) complex VO(OtBu)(OtBu)(OOtBu) turns out to be energetically the most favorable compound (indicated in the bottom right of **Figure 10b**). Any complex of family **12** formed during the catalytic cycle will finally evolve to the complex where all passive ligands are replaced by OtBu. These ligand exchange reactions require the presence of *tert*-butanol, but since the concentration of this alcohol is systematically increasing with reaction time, theory will predict complex VO(OtBu)(OtBu)(OOtBu) as the most abundant active species, and this is in complete agreement with experimental observations.

The same conclusion cannot entirely be drawn for the vanadium +IV complexes. The scheme in **Figure 10a** predicts VO(acac)(OOtBu) and V(OH)(OtBu)(acac)(OOtBu) as most favorable active compounds. The complex with two OtBu ligands suffers from a slightly higher free energy of about 25 kJ/mol, which is still reasonable. The corresponding VO(OtBu)(OOtBu) alkylperoxo complex with a V=O ligand is substantially higher activated (about 50 kJ/mol). It confirms that in the first catalytic cycle, active species with a bidentate ligand coordinating to vanadium V^{+IV} are present in this complex mechanism of subsequent epoxidation and activation processes. This is partly also the case in the catalytic cycle with V^{+V} as active species, but less significant. In the vanadium +V complexes there is clear ligand preference for *tert*-butanol. The gain in free energy with respect to the other ligands amounts to 20 kJ/mol or more. On the other hand, within the complexes coordinated with TBHP (compound family **17**), the bidentate ligands (acac and OAc) turn out to be the most favorable ligands.

Another relevant remark resulting from experimental work is the strong preference of acetic acid for coordination with vanadium. Theoretically, this preference is not that pronounced but it cannot be excluded on energetic grounds. In addition, further ligand exchange reactions on complexes containing acac ligands with water or *tert*-butanol will release Hacac, which is not stable against oxidation and rapidly oxidizes towards acetate acid and release of CO₂ gas. With increasing reaction time, the appearance of OAc-containing active vanadium complexes in the reagent mixture will obviously grow.

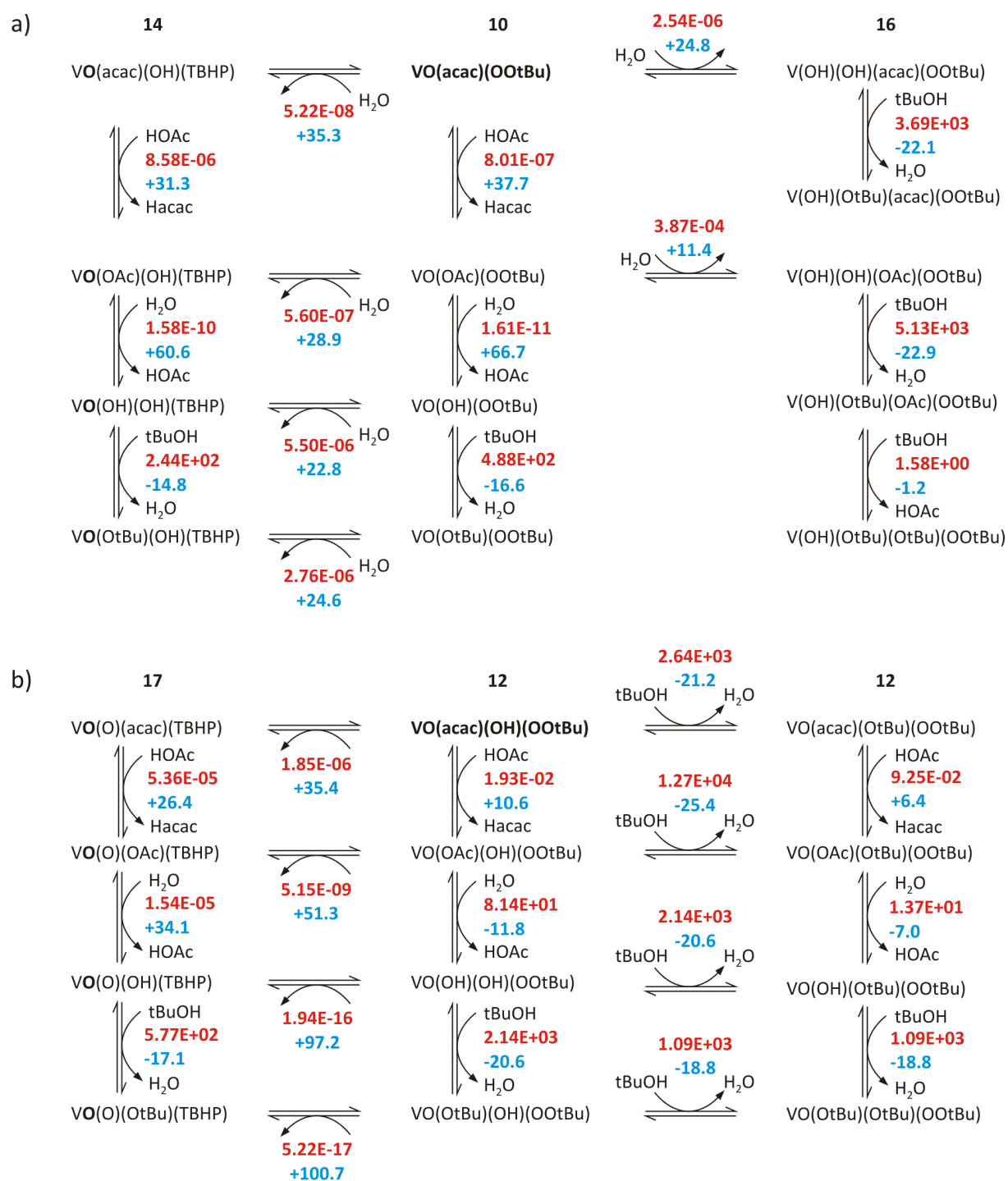


Figure 10: a) Scheme displaying a selection of equilibrium steps between active V^{+IV} epoxidation complexes of the type **14**, **10** and **16**($L_3=OH$). Complex $VO(acac)(OObu)$ is taken as the reference for the indication of the free energies and is indicated in bold. b) Equilibriums between active V^{+V} epoxidation complexes of the type **17** and **12**. Complex $VO(acac)(OH)(OObu)$ is taken as the reference for the indication of the free energies and is indicated in bold. The equilibrium coefficients $K_p(T)$ are indicated in red belonging to a temperature of 323 K. Also the Gibbs free energy differences ΔG_{323K} (in kJ/mol) are reported (blue). All data were calculated on the B3LYP/6-311+g(3df,2p)-D3 level of theory for the energetics.

5.2 Equilibrium between inactive complexes (IC)

Similarly as for the active complexes, equilibriums between inactive complexes have also been investigated. A scheme similar as **Figure 10** has been constructed based on the different equilibrium steps displayed in **Figure 5a**. As it does not reveal new conclusions fundamentally different from those drawn for the active species, the scheme is taken up in the S.I. under **Figure S.4**. The Gibbs free energy differences are listed for each path on the surface of inactive complexes and are of practical use to extract the Gibbs free activation energy required for activating any inactive species to a specific active species. The procedure will be outlined in the remainder of the paper.

5.3 Activation from inactive to active complexes

Inactive complexes are activated to active complexes after reaction with TBHP. The different classes are depicted in **Figure 4**. These activation reactions are described as equilibrium steps. In the early stages of epoxidation also the reaction given in **Figure 2** where the $VO(acac)_2$ catalyst is activated with TBHP is relevant. This equilibrium step belongs to the class **13** + TBHP \rightarrow **10** + HL_2 (**Figure 4**). A Gibbs free energy difference of +44.5 kJ/mol is found at 323 K, but since Hacac oxidizes fastly with a strong exothermic reaction energy of -1171 kJ/mol, the reaction becomes irreversible. Acetate acid - one of the end products of the oxidation of Hacac - will grow in importance in the reagent mixture and hence in ligand exchange reactions between the various vanadium complexes.

The Gibbs free energies differences between active complex and inactive complexes at 323 K are tabulated in the first two column of **Tables 3** and **4**, these will further be referred as activation free energies, i.e. $\Delta G_{323,act}$, referring to the activation step of inactive to active complexes. **Table 3** contains all vanadium species in oxidation state +IV whereas **Table 4** contains the species in oxidation state +V. Two inactive compounds are chosen as reference level for the activation free energies, i.e. $VO(acac)(OH)$ **13**($L_1=acac, L_2=OH$) and $V(OH)(Obu)(Obu)(Obu)$ **15** for the inactive V^{+IV} species and $VO_2(acac)$ **11**($L_1=acac$) and $VO(Obu)(Obu)(Obu)$ **18**($L_1=Obu, L_2=Obu, L_3=Obu$) for the inactive V^{+V} species. In the early stages of the reaction one could expect that inactive complexes with an acetyl acetate ligand will certainly be abundantly present in the reagent mixture (they are also energetically favored on the free energy surface (**Figure S.4**)). The second reference species are inactive complexes which will become more and more dominant in the course of the epoxidation reaction, due to the increasing amount of *tert*-butanol in the reagent mixture and the fact that these complexes are energetically the most favored on the Gibbs free energy surface at 323 K. A schematic figure representing the class of active and inactive complexes for the various oxidation states and the reference species is given in **Figure 11**.

Table 3: Free energies for activation steps from inactive to active complexes and kinetics for epoxidation reactions starting from active V^{+IV} complexes. The activation free energies $\Delta G_{323,act}^{IC1}$ and $\Delta G_{323,act}^{IC2}$ are referred to VO(acac)(OH) and V(OH)(OtBu)(OtBu)(OtBu), respectively and represent free energy differences between active and inactive complexes. $\Delta E_{0,app}^\ddagger$ and $\Delta G_{323,app}^\ddagger$ are the electronic activation energy for epoxidation reaction and the activation free energy for epoxidation as defined in **Figure 7**. $\Delta E_{0,r,app}$ and $\Delta G_{323,r,app}$ are the electronic energy differences between product and reactant of epoxidation including Zero point vibrational energies and the free energy differences between product and reactant of epoxidation at 323 K. Results are on the B3LYP/6-311+g(3df,2p)-D3 level of theory. All energies in kJ/mol.

	Activation Steps		Epoxidation Reactions				$k_{bi} \left(m^3 mol^{-1} s^{-1} \right)$	$\Delta G_{323,act+epox}^{IC1}$
	$\Delta G_{323,ac}^{IC1}$	$\Delta G_{323,act}^{IC2}$	$\Delta E_{0,app}^\ddagger$	$\Delta G_{323,app}^\ddagger$	$\Delta E_{0,r,app}$	$\Delta G_{323,r,app}$		
	13->14	15->14	reaction mechanism Ia					
VO(acac)(OH)—TBHP	-4.2	6.3	42.1	97.3	-174.2	-172.6	3.34E-05	93.1
VO(acac)(OtBu)—TBHP	-13.4	-3.0	45.9	103.3	-182.4	-180.8	3.49E-06	89.9
VO(OAc)(OH)—TBHP	27.1	37.6	31.5	86.6	-188.6	-186.8	1.77E-03	113.8
VO(OAc)(OtBu)—TBHP	17.4	27.8	33.7	90.2	-196.4	-195.8	4.67E-04	107.6
VO(OH)(OH)—TBHP	87.8	98.2	22.0	74.9	-248.7	-249.0	1.36E-01	162.7
VO(OtBu)(OH)—TBHP	73.0	83.4	20.2	76.0	-252.8	-249.5	9.21E-02	149.0
VO(OtBu)(OtBu)—TBHP	60.1	70.5	20.3	76.5	-256.4	-252.6	7.51E-02	136.6
	13->14	15->14	reaction mechanism Ib					
VO(acac)(OH)—TBHP	-25.9	-15.4	36.9	92.0	-171.3	-170.0	2.36E-04	66.2
VO(acac)(OH)—TBHP endo	-25.9	-15.4	37.5	92.4	-171.3	-170.0	2.01E-04	66.6
VO(acac)(OtBu)—TBHP	-30.8	-20.3	41.3	98.7	-182.4	-181.5	1.97E-05	67.9
VO(OAc)(OH)—TBHP	4.6	15.0	24.6	78.9	-113.8	-162.6	3.08E-02	83.5
VO(OAc)(OH)—TBHP radical	4.6	15.0	25.1	78.8	-122.4	-126.9	3.23E-02	83.4
VO(OAc)(OtBu)—TBHP	-4.6	5.8	26.6	85.0	-94.2	-153.4	3.21E-03	80.4
VO(OH)(OH)—TBHP	66.4	76.9	-0.5	38.5	-195.4	-197.3	1.06E+05	104.9
	13->10	15->10	reaction mechanism IIa					
VO(acac)(OOtBu)	-39.4	-29.0	14.6	68.4	-152.6	-159.3	1.55E+00	29.0
VO(OAc)(OOtBu)	-1.7	8.7	8.9	61.4	-151.7	-156.3	2.09E+01	59.7
VO(OH)(OOtBu)	65.0	75.4	7.9	58.4	-146.9	-154.3	6.46E+01	123.4
VO(OtBu)(OOtBu)	48.4	58.8	8.6	59.8	-147.8	-157.0	3.77E+01	108.2
	13->16	15->16	reaction mechanism IIb					
V(OH)(acac)(OH)(OOtBu)	-14.6	-4.2	82.5	143.5	-116.2	-167.5	1.12E-12	128.9
V(OH)(acac)(OtBu)(OOtBu)	-36.7	-26.2	100.3	164.6	-106.4	-162.1	4.29E-16	127.9
V(OH)(OAc)(OH)(OOtBu)	9.6	20.0	78.8	139.3	-99.7	-150.0	5.25E-12	148.9
V(OH)(OAc)(OtBu)(OOtBu)	-13.3	-2.9	91.8	154.6	-90.8	-144.7	1.78E-14	141.3

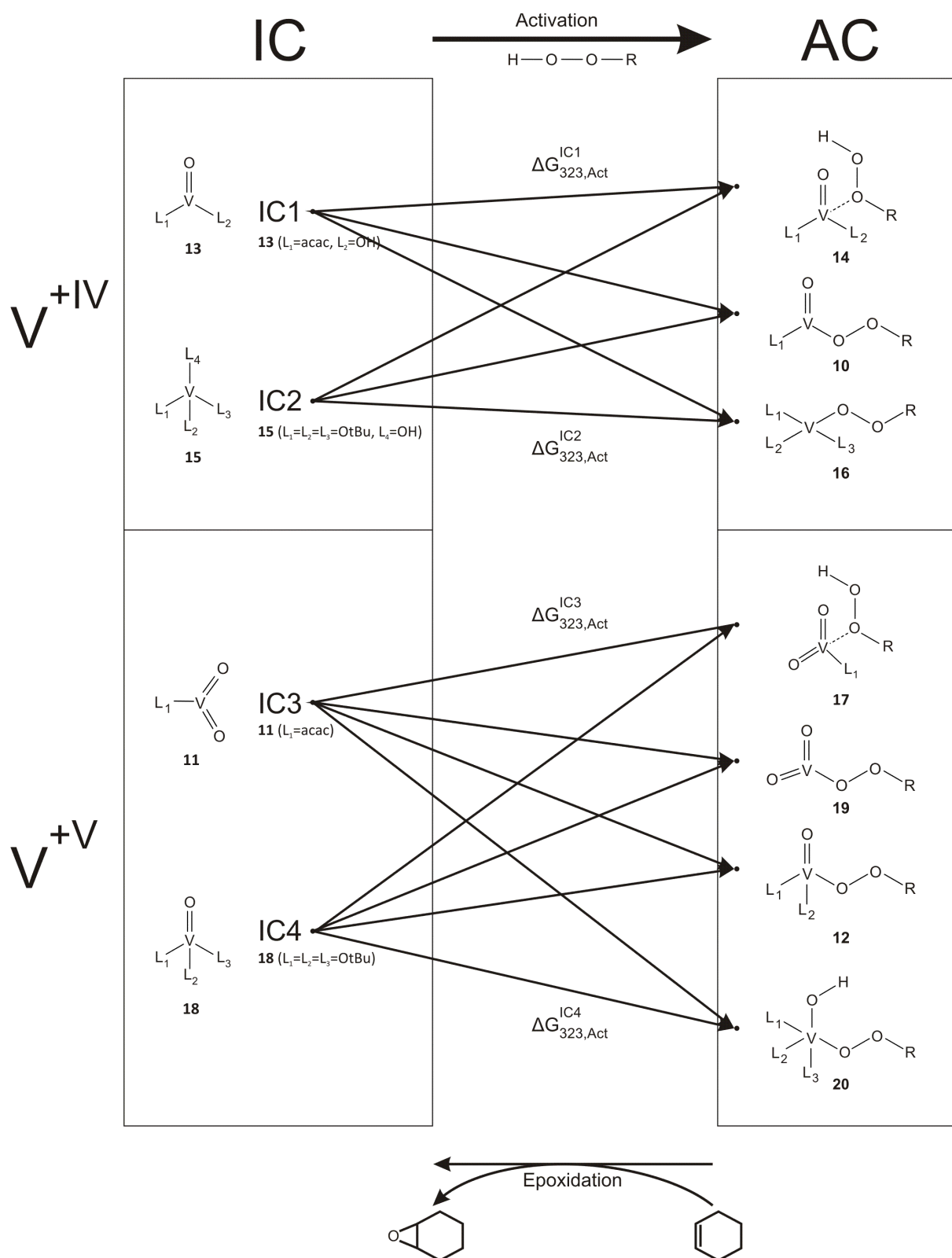


Figure 11: Schematic representation of the class of active and inactive complexes for the various oxidation states and the reference species, IC1, IC2, IC3 and IC4 are defined as VO(acac)(OH), V(OH)(OtBu)(OtBu)(OtBu), VO₂(acac) and VO(OtBu)(OtBu)(OtBu).

To obtain a complete picture of the activation process, only one activation free energy is needed together with the free energy differences among all active and inactive complexes. For example to

activate the reference inactive complex VO(acac)(OH) **13** ($L_1=acac, L_2=OH$) (which will be called IC1) to the corresponding activated complex VO(acac)(OH)-TBHP **14** a free energy difference of -4.2 kJ/mol is obtained (first line **Table 3**). With the additional knowledge of the free energy differences between the various inactive complexes and active complexes a complete picture of all transformations between inactive and active complexes can be obtained. The activation free energies tabulated in **Table 3** and **4** represent actually the Gibbs free energy difference required for activating reference compound IC1 to any active complex ACi after reaction with TBHP. Summarizing, knowledge of the Gibbs free energy surfaces corresponding to the respective inactive (**Figure S.4**) and active complexes (**Figure 10**) and knowledge of only one activation step are sufficient to construct the entire energy balance for each active species ready for epoxidation.

Table 4: Free energies for activation steps from inactive to active complexes and kinetics for epoxidation reactions starting from active V^{+V} complexes. The activation free energies $\Delta G_{323,act}^{IC3}$ and $\Delta G_{323,act}^{IC4}$ are referred to VO₂(acac) (IC3) and VO(OtBu)(OtBu)(OtBu) (IC4), respectively and represent free energy differences between active and inactive complexes. $\Delta E_{0,app}^\ddagger$ and $\Delta G_{323,app}^\ddagger$ are the electronic activation energy for epoxidation reaction and the activation free energy for epoxidation as defined in **Figure 7**. $\Delta E_{0,r,app}$ and $\Delta G_{323,r,app}$ are the electronic energy differences between product and reactant of epoxidation including Zero point vibrational energies and the free energy differences between product and reactant of epoxidation at 323 K. Results are on the B3LYP/6-311+g(3df,2p)-D3 level of theory. All energies in kJ/mol.

	$\Delta G_{323,act}^{IC3}$	$\Delta G_{323,act}^{IC4}$	$\Delta E_{0,app}^\ddagger$	$\Delta G_{323,app}^\ddagger$	$\Delta E_{0,r,app}$	$\Delta G_{323,r,app}$	$k_{bi} \left(m^3 mol^{-1} s^{-1} \right)$	$\Delta G_{323,act+epox}^{IC3}$
	11->17	18->17	reaction mechanism Ia					
VO(O)(acac)—TBHP	-9.3	85.6	39.1	94.2	-214.6	-212.4	1.05E-04	84.9
VO(O)(acac)—TBHP endo	-9.3	85.6	35.2	91.6	-214.6	-212.4	2.71E-04	82.4
VO(O)(OAc)—TBHP	17.1	112.0	22.1	78.9	-246.5	-245.3	3.15E-02	96.0
VO(O)(OAc)—TBHP endo	17.1	112.0	17.3	75.2	-246.5	-245.3	1.22E-01	92.4
VO(O)(OH)—TBHP	51.2	146.1	8.9	59.9	-286.9	-287.9	3.62E+01	111.2
VO(O)(OH)—TBHP endo	51.2	146.1	1.4	54.6	-176.1	-179.3	2.66E+02	105.8
VO(O)(OtBu)—TBHP	34.2	129.0	8.8	61.9	-289.1	-288.4	1.74E+01	96.1
VO(O)(OtBu)—TBHP endo	34.2	129.0	2.2	56.3	-289.1	-288.4	1.39E+02	90.5
	11->17	18->17	reaction mechanism Ib					
VO(O)(OAc)—TBHP	26.7	121.6	7.2	64.3	-205.8	-198.8	7.21E+00	91.0
VO(O)(OH)—TBHP	58.4	153.3	-0.4	52.2	-183.6	-186.5	6.55E+02	110.6
VO(O)(OtBu)—TBHP	43.7	138.6	1.0	52.8	-202.8	-202.1	5.15E+02	96.6
	11->12	18->12	reaction mechanism IIa					
VO(acac)(OH)(OOtBu)	-44.7	50.2	48.8	108.7	-185.8	-184.1	4.74E-07	64.0
VO(acac)(OtBu)(OOtBu)	-65.9	29.0	47.7	109.5	-178.7	-174.7	3.47E-07	46.8
VO(OAc)(OH)(OOtBu)	-34.1	60.7	22.2	80.9	-192.3	-190.9	1.47E-02	57.1
VO(OAc)(OAc)(OOtBu)	-21.2	73.6	14.3	78.3	-195.6	-197.7	3.85E-02	34.0
VO(OAc)(OtBu)(OOtBu)	-59.5	35.4	34.5	93.50	-192.4	-189.2	1.36E-04	56.3
VO(OH)(OH)(OOtBu)	-46.0	48.9	49.2	102.3	-190.0	-190.7	5.06E-06	41.2
VO(OtBu)(OH)(OOtBu)	-66.5	28.4	48.5	107.7	-188.4	-187.7	6.82E-07	31.0
VO(OtBu)(OtBu)(OOtBu)	-85.3	9.6	53.9	116.3	-188.4	-191.7	2.80E-08	43.6

	11->12	18->12	reaction mechanism IIb					
VO(OH){acac}(OOtBu)	-44.7	50.2	107.6	168.6	-88.3	-137.4	9.64E-17	123.9
VO(OH)(OAc)(OOtBu)	-34.1	60.8	103.1	162.1	-30.8	-79.8	1.07E-15	128.0
VO(OH)(OH)(OOtBu)	-45.9	48.9	120.9	175.2	77.8	25.8	8.19E-18	129.3
VO(OH)(OtBu)(OOtBu)	-66.5	28.4	125.9	181.9	80.4	24.8	6.94E-19	115.3
	11->	18->	reaction mechanism III					
VO(OO)(OOtBu) 22	26.7	121.6	7.8	58.2	-155.9	-159.2	1.39E+02	84.9
VO ₂ (OOtBu) 19	97.1	192.0	-9.0	41.7	-134.2	-136.8	6.46E+04	138.8
VO(OO)(OH) 21 (L ₁ =OH)	73.5	168.4	11.1	59.9	-95.4	-93.6	7.32E+01	133.4
VO(OO)(OtBu) 21 (L ₁ =OtBu)	49.6	144.5	15.8	66.8	-89.9	-89.3	2.79E+00	116.4

In order to determine the fastest epoxidation reaction mechanism, we need a complete energetic balance of all active compounds, which can be deduced following the procedure explained in **Figure 11**. However, not all equilibria are displayed on the Gibbs free energy surfaces for active complexes (**Figure 10**). The two highly active peroxy vanadium complexes VO(OO)(OH) **21**(L₁=OH) and VO(OO)(OOtBu) **22** are not taken up in the general scheme of **Figure 4** but may result from active dioxo V^{+V} complexes, such as complexes **17** and **19**. An example of a possible mechanism to these active peroxy complexes is demonstrated in **Figure 12**. The scheme starts from the active dioxo V^{+V} complex **17** VO(O)(OH)-TBHP that transforms into the peroxy complex **21**(L₁=OtBu) after spatial reorientation of the coordinated TBHP and release of water. In general complexes **17** and also complex **21** VO(OO)(OH) are substantially higher in energy than the most stable active complex (VO(OtBu)(OtBu)(OOtBu)) with energy differences of the order of 150 kJ/mol. In order to make these active species and subsequent epoxidation reaction plausible in the overall reaction scheme, a substantial higher epoxidation rate would be required. We will discuss these issues in following section.

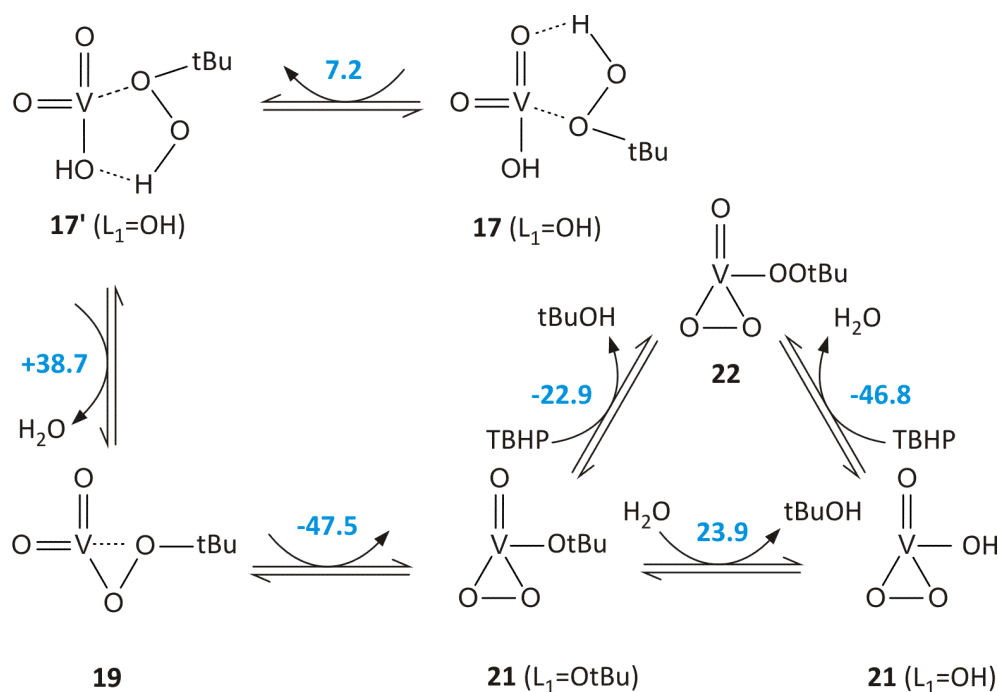


Figure 12: A plausible pathway starting from an abundant V^{+V} inactive complex **18** to the highly activated peroxy complex **21**. The Gibbs free energy differences (in kJ/mol) of the displayed equilibria are reported in blue belonging to a temperature of 323 K.

Careful inspection of the activation free energies for both V^{+IV} complexes coordinated with TBHP learns that the formation of active complexes ready for epoxidation pathways **Ib** are preferred over **Ia** and formation of some active complexes ready for pathways **IIa** and **IIb** are also preferred over **Ia**. For V^{+V} complexes, there is clearly a preference for formation of active complexes of epoxidation pathways **IIa** en **IIb**. However to make conclusions about the preferred epoxidation pathways, also Gibbs free energy barriers for epoxidation need to be taken into consideration.

5.4 Epoxidation reactions

Epoxidation transition states have been theoretically modeled for each active species and the various reaction mechanisms proposed in **Figure 4**. 3-D representations of the transition states are shown in **Figure 13**. In **Tables 3** and **4** the apparent kinetic data are taken up, i.e. where the reference level is taken as the active vanadium complex and cyclohexene in the gas phase. For sake of completeness we also report the unimolecular kinetic data in **Tables S.3** and **S.4** of the Supporting Information. The list of active species is almost complete and comprises all ligand combinations with exception of twice the acac and OAc ligands in the same mono-vanadium complex. In this context it is also worthwhile to note that even an excess of TBHP will never restore $VO(acac)_2(OOtBu)$ as active complex, fully in line with the experimental findings reported by Talsi [8], due to the irreversible oxidation of the acac ligand into acetic acid.

Inspection of the **Tables 3** and **4** learns that the energy barriers may vary drastically going from nearly zero to about 130 kJ/mol. To discriminate between plausible epoxidation pathways, taking into account both the abundance of the active species and the rate constant for epoxidation, we introduced a global free energy barrier ($\Delta G_{323,act+epox}^{IC1}$) that is defined as the sum of the activation free energy ($\Delta G_{323,act}^{IC1}$) and the epoxidation free energy barrier ($\Delta G_{323,app}^\ddagger$). For V^{+V} species a similar quantity $\Delta G_{323,act+epox}^{IC3}$ is introduced.

Within the class of V^{+IV} complexes, species $VO(acac)(OOtBu)$ appears as one of the favorable active complexes ($\Delta G_{323,act}^{IC1} = -39.4$ kJ/mol), which furthermore has one of the lowest activation free energy barriers for epoxidation ($\Delta G_{323,app}^\ddagger = 68.4$ kJ/mol) or a bimolecular epoxidation rate of $1.55 \text{ m}^3 \text{ mol}^{-1} \text{ s}^{-1}$. This favorable reaction cycle falls into the class of the Sharpless reaction mechanism **IIa**, and will be one of the dominant reaction paths for epoxidation of cyclohexene over $VO(acac)_2$ catalysts. This is certainly the case in the early stages of the epoxidation process, but since any release of Hacac in a ligand exchange reaction will irreversibly transform the acetyl acetonate acid into acetate acid this reaction path will decrease in importance. Within the same reaction family also species $VO(OAc)(OOtBu)$ results in a low global free energy barrier for epoxidation ($\Delta G_{323,act+epox}^{IC1} = 59.7$) and will generate favorable epoxidation paths.

On basis of our kinetic and thermodynamic data, reaction mechanism **IIb** is ruled out as a probably reaction cycle for epoxidation. This is an immediate result from the high (free) energy barriers for epoxidation. The active complexes of the type **16** for V^{+IV} (and also type **12** for V^{+V} (see **Figure 3**) have not the most ideal configuration to epoxidize the double bond in cyclohexene, although their free energies for formation predict a relatively high abundance. Also the reaction mechanism **Ia** are not regarded as very plausible cycles for epoxidation.

To a large extent the same conclusions can be drawn for the class of the V^{+V} complexes: reaction mechanism **IIb** exhibits extremely low reaction rates despite the high probability for the formation of active complexes leading to this route, while the most preferred epoxidation mechanism is manifestly **IIa** with total free energies of activation + epoxidation that vary between 31 and 64 kJ/mol, which is by far 30 kJ/mol lower in energy than all other $\Delta G_{323,act+epox}^{IC3}$ predictions. When studying the values within this class in more details, it becomes apparent that the reaction rates for epoxidation may vary substantially with orders of magnitude depending on the choice of the ligands L_1 and L_2 in the active complex family $VO(L_1)(L_2)(OOtBu)$ **12**. It is striking that acetyl acetate and OtBu ligands hinder the epoxidation with low rate constants around $10^{-7} \text{ m}^3\text{mol}^{-1}\text{s}^{-1}$ despite their thermodynamical assignment as most favorable V^{+V} complexes (**Figure 10** and first column of **Table 4**). Largest reaction rates (of about $10^{-2} \text{ m}^3\text{mol}^{-1}\text{s}^{-1}$) correspond with species containing the acetate ligand. Those complexes are thermodynamically slightly less favorable than the former with OtBu ligands, but the large reaction rate constant largely compensates this effect. The corresponding transition state is also shown in **Figure 13**. Furthermore, this means that acetic acid can also be added experimentally to the solution, to fasten the epoxidation reaction, hereby confirming previous experimental studies on the acceleration effect of acetic acid [59, 60].

The reaction mechanisms **Ia** and **Ib** use TBHP coordinated complexes. The individual reaction rates for epoxidation of complexes of family **17** are relatively high. Also here acetate as ligand predicts the highest rate constant within this **Ia** reaction mechanism (see **Table 2**). However, thermodynamically the formation of the active complexes is not preferred especially compared to the active complexes of family **12**. Although, species of the type **17** are also formed via radical decomposition from active V^{+IV} coordinated complexes of type **14** following the mechanism outlined in **Figure 3**. In this respect $VO(O)(L_1)(TBHP)$ **17** complexes can be more present than predicted according to the equilibrium steps sketched in **Figure 10**. More information about the radical decomposition steps will be given further in this paper.

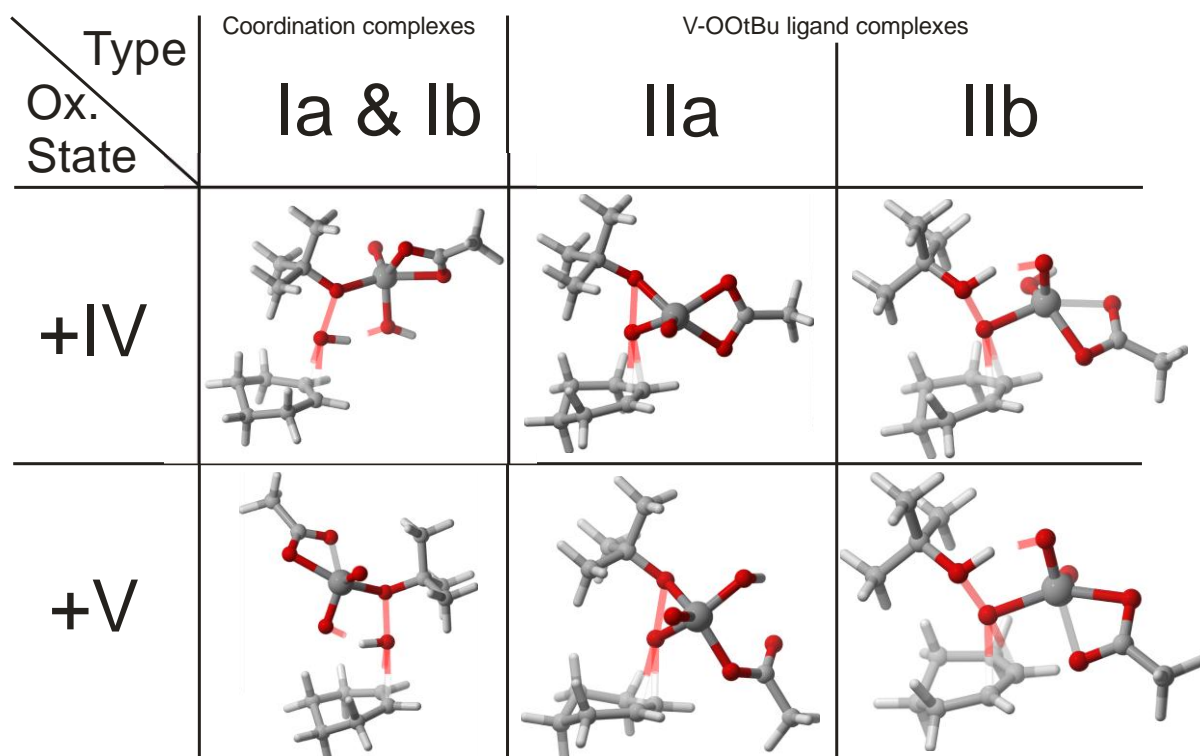


Figure 13: Transition states for the mechanism types I and II with acetate ligands.

For complexes **17** involved in the reaction mechanisms **Ia** and **Ib**, several transition states were possible that mainly differ in the stereochemical position of the ligands on the active complexes. We calculated transition states with an *endo* or *exo* position of the coordinated cyclohexene with respect to the vanadium dioxocompound. They are illustrated in **Figure S.5** in the Supporting Information. The *endo*-TS predicts a slightly smaller energy barrier (**Table 4**), but does not alter the overall conclusions.

Epoxidations according to mechanism **III** which start from peroxy species of type **19**, **21** or **22** are characterized by a high rate of epoxidation. This is especially true for the peroxy complex $\text{VO}_2(\text{OOtBu})$ **19** which has actually the highest rate of epoxidation ($6.4\text{E}+04 \text{ m}^3/\text{mol/s}$). Some characteristic transition states are given in **Figure 14**. Apart from the possible mechanism given in **Figure 12** for formation of these active complexes, also other routes produce peroxovanadium species from the reaction of TBHP with the oxometal group of the catalyst, as proposed for example by Chong and Sharpless [44]. Although thermodynamically the formation of these complexes is not favored, as already mentioned earlier. For example the Gibbs free energy difference between species **19** and the most stable species $\text{VO}(\text{OtBu})(\text{OtBu})(\text{OOtBu})$ amounts to 182.5 kJ/mol, which can readily be deduced from the equilibrium steps displayed in **Figures 10** and **12**. As such overall mechanism **III** is not preferred with global free energies ($\Delta G_{323,\text{act+epox}}^{\text{IC3}}$) amounting to about 130 kJ/mol.

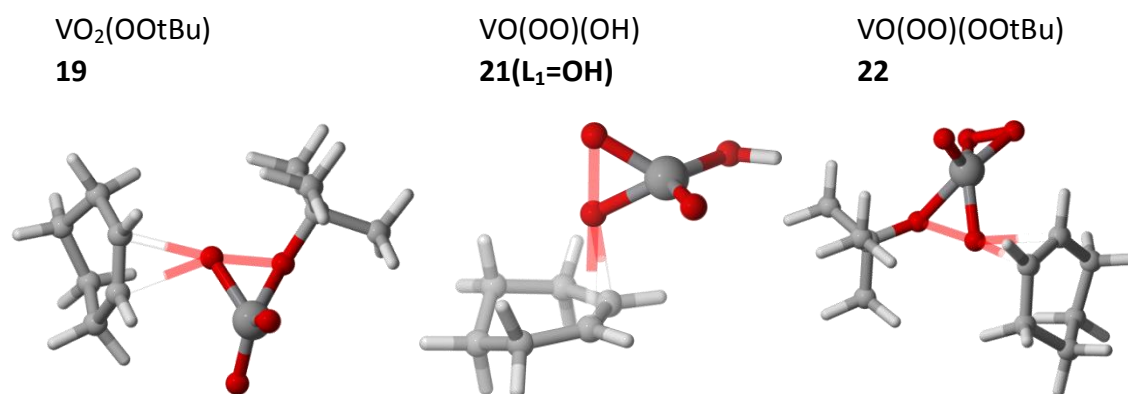


Figure 14: Transition states for epoxidation starting from peroxy complexes

Finally, the major end product of the epoxidation reaction in the vanadium/TBHP catalytic system is *tert*-butanol beside the cyclohexene oxide. On the other hand *tert*-butanol is also involved in multiple ligand exchange reactions on both inactive and active equilibrium free energy surfaces. As the reaction time increases high yields of tBuOH will be observed and will prevail in the reagent mixture, leading to less active species.

5.4 Coordination with water and *tert*-butanol

All equilibrium reactions on the Gibbs free energy surfaces for active and inactive complexes, displayed in **Figure 10** and **Figure S.4**, and activation reactions (IC→AC) are modeled without coordination with water or *tert*-butanol. They could heavily affect the Gibbs free energy of the exchange ligand reactions or others, but the overall picture will not be affected. To illustrate with an example we concentrate on the activation step from the inactive complex $\text{VO}(\text{OH})(\text{OH})(\text{OH})$ **18** to the active complex $\text{VO}_2(\text{OH})$ -TBHP **17**. Without coordination with water – following the lines as applied in the previous sections – the Gibbs free energy difference between $\text{VO}(\text{OH})(\text{OH})(\text{OH})$ **18** and IC4 amounts to -61.2 kJ/mol (can be readily deduced from the Gibbs free energy surface in **Figure S.4**). **Table 4** learns that activation of IC4 to active complex $\text{VO}_2(\text{OH})$ -TBHP **17** requires an energy of 146.1 kJ/mol. **Figure 15** describes the same activation step from $\text{VO}(\text{OH})(\text{OH})(\text{OH})$ to $\text{VO}_2(\text{OH})$ -TBHP **17** but now via species **11** coordinated with water. This path leads to the same result. But we also learn that the complex **11**(L₁=OH) coordinated with water is of about 100 kJ/mol more bound than the uncoordinated complex. Summarizing, a whole description with each complex coordinated with water or *tert*-butanol will not alter the conclusions made in the previous sections. We have preferred to not take them into consideration, as they will disturb the transparency of the discussion.

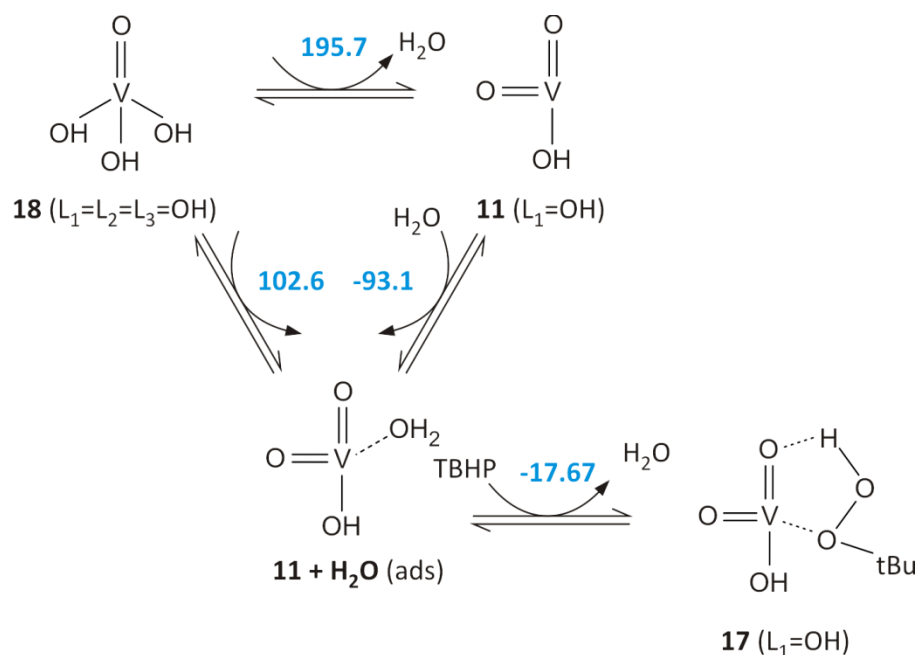


Figure 15: Activation of the complex $\text{VO}(\text{O})(\text{OH})$ coordinated with water to active complex $\text{VO}(\text{O})(\text{OH})$ coordinated with TBHP.

5.5 Radical decomposition reactions

In the previous discussion, $\text{V}^{+\text{IV}}$ and $\text{V}^{+\text{V}}$ species were treated as two independent families that could undergo epoxidation. However they can mutually transform into each other by radical decomposition reactions, as already illustrated in **Figure 3**. The $\text{V}^{+\text{IV}} \rightarrow \text{V}^{+\text{V}}$ oxidation happens by production of $\text{tBuO}\bullet$ radicals, while the reverse transfer takes place by production of $\text{tBuOO}\bullet$ radicals.

Some catalytic cycles for the interconversion of +IV and +V vanadium species were already investigated for the above mentioned Vanadate/PCA system [34]. The proposed mechanism for radical generation with TBHP is completely analogous as that applied in this work (**Figure 3**).

Table 5 gives an overview of reaction energies and reaction kinetics for the various radical decomposition reactions displayed in **Figure 3**. We first concentrate on the generation of the $\text{tBuO}\bullet$ radical yielding $\text{V}^{+\text{V}}$ species. The reaction energies show a strong dependence on the ligand choice. With an acac ligand in the complex the reaction is thermodynamically favored for the formation of $\text{tBuO}\bullet$ giving a reaction free energy of -22 kJ/mol whereas with all other ligands this value becomes positive. These results are in agreement with our earlier published data, where a vanadium cluster with two terephthalate linkers was used to simulate the MIL-47 framework [11]. In that case a reaction free energy was calculated of -34.7 kJ/mol. For monodentate ligands such as the hydroxyl and *tert*-butoxide anion the reaction takes values of about 35 kJ/mol. The observed trends can be related to the type of coordination of bidentate and monodentate ligands. The first one is tetrahedrally coordinated in the vanadium $\text{VO}_2(\text{L})$ complex and are more stabilized with respect to trigonal planar coordinated species. On the other hand the electronic activation barrier for the cleavage of the peroxide bond varies only slightly in terms of other ligands with values ranging from 30 to 40 kJ/mol. The reason for the apparently different behavior of the reaction energy should rather be searched in the different spatial coordination of the ligand with the metal. One should however be careful in analyzing the exact values for the free energies for the radical decomposition reaction $\text{VO}(\text{L}_1)(\text{O}(\text{O}t\text{Bu})) \rightarrow \text{VO}_2(\text{L}_1) + \text{tBuO}\bullet$, as in reality these reactions take place in a reagent

mixture with solvent, water, acids, alcohols, etc. If we reexamine the above reaction but now with the product coordinated with water, the reaction energy becomes negative in all cases. If we start from an already water coordinated species $\text{VO}(\text{L}_1)(\text{OOtBu})(\text{H}_2\text{O})$ forming the coordinated $\text{VO}_2(\text{L}_1)(\text{H}_2\text{O})$, the reaction energy is still exothermic ($\Delta G_{323,r,app} = -42.4$ kJ/mol for $\text{L}_1=\text{OH}$) whereas the electronic barrier remains nearly the same (31.8 kJ/mol). These results indicate the reaction is thermodynamically driven if coordinating ligands are present.

Summarizing, the obtained thermodynamic and kinetic data confirm that in all stages of the epoxidation reactions the transformation $\text{V}^{+IV} \rightarrow \text{V}^{+V}$ will certainly take place.

Apart from the transformation from $\text{V}^{+IV} \rightarrow \text{V}^{+V}$ species through oxidation, also V^{+V} species may transform back into V^{+IV} complexes (**Figure 3b**). In Leus and Vandichel et al. [11], it has been found that the reaction free energy for this step is competitive (around 37 kJ/mol) with epoxidation reactions. In **Table 5** we also report the reaction energies, but in contrast to the MIL-47 cluster these “recycling” reactions become less probable when bidentate ligands are replaced by monodentate ligands. With the systematic increase of *tert*-butanol in the reagent mixture together with the decrease of Hacac, we could expect that the transformation of V^{+V} to V^{+IV} species will mainly occur during the early stages of the epoxidation, but that this recycling process will become less important as the reaction proceeds. We also investigated the effect of the coordination with water on the reaction free energies in the process $\text{V}^{+V} \rightarrow \text{V}^{+IV}$. In contrast to the $\text{V}^{+IV} \rightarrow \text{V}^{+V}$ radical decomposition this has little influence on the thermodynamics. If the transformation would take place, it is most preferred for complexes with acac ligands. As these ligands are also readily consumed during the reaction cycle by oxidation (**Figure 2**), the probability of going back to the oxidation state +IV is less probable as the reaction proceeds.

With the generation of $\text{tBuOO}\bullet$ radicals in the catalytic cycle highly active species are formed which can epoxidize cyclohexene following the so-called Twigg mechanism [61]. We did the calculation and found that the Twigg epoxidation mechanism turned out to be not favorable: first an intermediate of alkoxy radical type is formed with a high reaction free energy barrier of 92.4 kJ/mol and finally the epoxidation with a barrier of 30.3 kJ/mol. In view of these findings this specific epoxidation path can be seen as a minor route toward cyclohexene oxide. The interested reader is referred to our earlier work [11] for more details on this mechanism.

Table 5: Radical decomposition following scheme given in **Figure 3a** and **3b**. ΔE_0^\ddagger and ΔG_{323}^\ddagger are the electronic reaction barrier and corresponding Gibbs free energy barrier. $\Delta E_{0,r,app}$ and $\Delta G_{323,r,app}$ are the electronic energy differences between products and reactant including Zero point vibrational energies and the corresponding Gibbs free energy differences at 323 K. Results are on the B3LYP/6-311+g(3df,2p)-D3 level of theory. All energies in kJ/mol.

$\text{V}^{+IV} \rightarrow \text{V}^{+V}$				
$10 \rightarrow 11 + \text{tBuO}\bullet$				
$\text{VO}(\text{L}_1)(\text{OOtBu}) \rightarrow \text{VO}_2(\text{L}_1) + \text{tBuO}\bullet$				
L_1	ΔE_0^\ddagger	ΔG_{323}^\ddagger	$\Delta E_{0,r,app}$	$\Delta G_{323,r,app}$
acac	38.5	38.8	33.6	-22.2

OAc	38.4	33.5	62.8	8.3
OH	30.9	31.3	90.3	35.3
OtBu	29.6	30.4	85.8	30.4
$\text{VO}(\text{L}_1)(\text{OOtBu}) + \text{H}_2\text{O} \rightarrow \text{VO}_2(\text{L}_1)(\text{H}_2\text{O}) + \text{tBuO}\bullet$				
acac			-9.4	-24.4
OAc			-18.3	-30.6
OH			-44.4	-57.8
OtBu			-45.3	-56.0
$\text{VO}(\text{L}_1)(\text{OOtBu})(\text{H}_2\text{O}) \rightarrow \text{VO}_2(\text{L}_1)(\text{H}_2\text{O}) + \text{tBuO}\bullet$				
OH	31.8	32.1	13.6	-42.4
OtBu	30.9	30.0	9.9	-47.8
$\text{V}^{+V} \rightarrow \text{V}^{+IV}$				
$\mathbf{12} \rightarrow \mathbf{13} + \text{tBuOO}\bullet$				
$\text{VO}(\text{L}_1)(\text{L}_2)(\text{OOtBu}) \rightarrow \text{VO}(\text{L}_1)(\text{L}_2) + \text{tBuOO}\bullet$				
L_1	L_2		$\Delta E_{0,r,app}$	$\Delta G_{323,r,app}$
acac	OtBu		135.3	72.1
OAc	OtBu		167.0	106.4
OH	OtBu		248.3	182.2
OtBu	OtBu		253.7	181.6
$\mathbf{12} + \text{H}_2\text{O} \rightarrow \mathbf{13} - \text{H}_2\text{O} + \text{tBuOO}\bullet$				
$\text{VO}(\text{L}_1)(\text{L}_2)(\text{OOtBu}) + \text{H}_2\text{O} \rightarrow \text{VO}(\text{L}_1)(\text{L}_2)(\text{H}_2\text{O}) + \text{tBuOO}\bullet$				
Acac	OtBu		86.7	75.0
OAc	OtBu		111.4	99.1
OH	OtBu		184.8	167.1
OtBu	OtBu		192.1	167.7

5.6 Comparison with experiment

The free energy barrier ($\Delta G^\ddagger = \Delta H^\ddagger - T.\Delta S^\ddagger$) for experimental epoxidation is estimated to be 79.9 ± 4.2 kJ/mol (323 K) by Gould *et al.* [4], obtained from fitting specific rate constants k (s^{-1}) at different temperatures. The value of 72.6 kJ/mol, obtained in our experimental study, closely resembles the Gould estimate [4] and appears to be in good agreement with some free energy barriers reported in **Tables 3** and **4**. However, it should be verified if the active vanadium complexes, predicting correct epoxidation reaction rates, can indeed be formed on thermodynamical grounds.

In order to validate the theory with experiment, we therefore consider two plausible routes toward epoxidation starting from the catalyst $\text{VO}(\text{acac})_2$ in its initial stage. In both plausible routes the epoxidation occurs via the **IIb** mechanism, which indeed was identified as the most plausible one. First we consider an example belonging to the family of V^{+IV} complexes, as they are probably present in the early stages of the reaction cycle. $\text{VO}(\text{acac})_2$ is an inactive complex of type **13** with two acetylacetonate linkers. At the early stage of the epoxidation process, activation of $\text{VO}(\text{acac})_2$ to $\text{VO}(\text{acac})(\text{OOtBu})$ with TBHP (as schematically shown in **Figure 2**) requires a Gibbs free energy of 44.5 kJ/mol which be easily composed after “traveling” over the IC surface (Figure S.4) to reach IC1 or IC2,

and by use of the activation energy as reported in Table 3. Afterwards species **10** VO(acac)(OOtBu) follows route **Ila** with an apparent free energy reaction barrier that amounts to 68.4 kJ/mol, which is in nice agreement with the experimental prediction, but thermodynamically the increase of 44.5 kJ/mol should be overcome. Initially this might occur through coupling with a highly exothermal reaction as the oxidation of Hacac. However, the subsequent epoxidation reaction, now starts from VO(acac)(OtBu) **13** as inactive species, which is then activated with formation of active species VO(acac)(OOtBu) and is preferred on the free energy surface by about -22.8 kJ/mol (easily deduced from **Figure S.4**). This means that as the catalytic cycle proceeds, this reaction path becomes more plausible and in agreement with experiment. Reaction mechanism **Ila** offers more active species, which in average give apparent free energies for epoxidation which are in close agreement with the experimental prediction.

The second example focuses on a V^{+V} complexes, which may be formed after a V^{+V} radical decomposition pathway. The pathway differs from the previous one in that VO(acac)(OOtBu) now oxidizes to VO₂(acac) (**11**(L₁=acac)) after reaction with TBHP with formation of tBuO• radical. It further undergoes an activation step to the desired active species VO(OAc)(OAc)(OOtBu) which corresponds to a free energy change of -21.2 kJ/mol. The required free energy barrier of 78.3 kJ/mol for epoxidation matches fairly well the experimental value.

Of course previous examples are indicative but demonstrate that the selected preferred reaction pathways, that all occur through mechanism **Ila** (the Sharpless mechanism) give free energies of epoxidation that are fairly close to the experimental values. On basis of our simulations we can not exclude the other pathways, as our model does not include any time dependence. It only evaluates the theoretical reaction rate and/or Gibbs free energy for any route which can take place. A kinetic model could be constructed based on some particular selection of plausible reaction routes and assumption of initial concentrations of all relevant ingredients. It falls, however, outside the scope of this work. Nevertheless, one can readily see that the favored pathways lead to an increased release of *tert*-butanol, which has a deactivating effect.

6 Conclusions

The epoxidation reaction of cyclohexene has been investigated theoretically for the system VO(acac)₂ with *tert*-butyl hydroperoxide. The overall reaction cycle consists of a variety of steps: first the catalyst needs to be brought into an active form through interaction with the oxidant, after that the epoxidation reaction might occur through a variety of possible reaction mechanisms. After that the catalyst is brought back into an inactive form and needs to be reactivated again through activation steps with the oxidant. This reaction cycle is valid both for vanadium species in oxidation state +IV and +V and change of oxidation state is also possible through radical decomposition reactions. In order to get a complete picture of the reaction cycle, the Gibbs free energies for all these hops among the various species have been modeled as thermodynamic equilibrium steps. As a result a free energy diagram was constructed for the various species bearing either oxidation state +IV and +V. The change in oxidation state was modeled through radical decomposition pathways for which also the kinetics was modeled. Our results show that the most abundant vanadium +IV species are VO(acac)(OOtBu), VO(acac)OtBu-TBHP and V(OH)(acac)(OtBu)(OOtBu) whereas for vanadium +V species complexes of the type VO(L₁)(L₂)(OOtBu) are energetically preferred. To draw conclusions on the actual epoxidation mechanisms, we calculated first principle chemical kinetics for a broad variety of earlier proposed epoxidation mechanisms. Our results show that for both oxidation states of

vanadium, the concerted Sharpless mechanism is preferred. This conclusion is made based on both the abundance of the active species ready for epoxidation along this pathway and their rate constant. For some species, high rate constants were found, this was particularly true for peroxy complexes of the type $\text{VO}_2(\text{OOtBu})$, but as there is a lot of free energy required to form these compounds, such reaction pathways are finally not preferred. The calculations do not reveal a particular ligand preference for monovanadium complexes leading to cyclohexene epoxidation, but the bidentate coordination of acetic acid (HOAc) with the vanadium catalyst is in most cases favorable.

Transitions from the V^{+IV} platform to V^{+V} platform and vice versa take place via radical decomposition pathways. Our calculations reveal that such transitions from V^{+IV} to V^{+V} complexes occur rather easily but the reverse transformation from V^{+V} to V^{+IV} complexes may only occur in the early stages of the catalytic epoxidation process due to the presence of Hacac as a ligand, required to keep the energy barrier low enough. With the systematic decrease of Hacac and herewith coupled increase of *tert*-butanol in the reagent mixture the recycling reaction bringing V^{+V} complexes back to coordination number +IV becomes seriously hindered. The calculations also reveal that the radicals $\text{tBuOO}\bullet$ and $\text{tBuO}\bullet$ produced during these radical decomposition reactions do not play a significant role in the epoxidation process of cyclohexene itself, but are dominant in the formation of by-products and in particular the adduct *tert*-butyl-2-cyclohexenyl-1-peroxide. Thus the so-called Twigg's mechanism where direct epoxidation occurs with the radical $\text{tBuOO}\bullet$ is not preferred.

A comparative study with similar calculations on Vanadium-MIL-47 catalysts learns that large similarities are observed, but also some significant differences. In particular the mutual $\text{V}^{+IV} - \text{V}^{+V}$ conversion in the entire catalytic cycle is more present in case of heterogeneous catalysis. And this is probably due to the more persistent presence of the terephthalate ligands in the active catalytic site.

This study is not able to give an accurate prediction of various species in function of the reaction time. Such study requires the initial concentrations of all ingredients in the reaction mixture and solving the microkinetic network of coupled reactions in function of the reaction time. In view of the huge number of plausible routes, such study falls outside the scope of this paper.

Acknowledgement :

This research is co-funded by the Ghent University, GOA grant nr. 01G00710, BELSPO in the frame of IAP 6/27 and the European Research Council (FP7(2007-2013) ERC grant nr. 240483). M. V. thanks the research board of Ghent University (BOF). K. L. is grateful to the Long Term Structural Methusalem grant nr. 01M00409 Funding by the Flemish Government. The authors would like to thank Ying-Ya Liu for her help and comments concerning the UV-Vis spectra. Computational resources and services were provided by Ghent University.

References

- [1] D.E. De Vos, B.F. Sels, and P.A. Jacobs, *Advances in Catalysis*, Vol 46. 1-87.
- [2] D.E. De Vos, B.F. Sels, and P.A. Jacobs, *Advanced Synthesis & Catalysis* 345 (2003) 457-473.
- [3] K.A. Jorgensen, *Chemical Reviews* 89 (1989) 431-458.

- [4] E.S. Gould, R.R. Hiatt, and K.C. Irwin, *Journal of the American Chemical Society* 90 (1968) 4573-&.
- [5] H.E.B. Lempers, A. Ripolles i Garcia, and R.A. Sheldon, *The Journal of Organic Chemistry* 63 (1998) 1408-1413.
- [6] C.K. Sams, and K.A. Jorgensen, *Acta Chemica Scandinavica* 49 (1995) 839-847.
- [7] L. Stepovik, and M. Gulenova, *Russ. J. Gen. Chem.* 79 (2009) 1663-1670.
- [8] E.P. Talsi, V.D. Chinakov, V.P. Babenko, and K.I. Zamaraev, *Journal of Molecular Catalysis* 81 (1993) 235-254.
- [9] K. Barthelet, J. Marrot, D. Riou, and G. Ferey, *Angewandte Chemie-International Edition* 41 (2002) 281-+.
- [10] K. Leus, I. Muylaert, M. Vandichel, G.B. Marin, M. Waroquier, V. Van Speybroeck, and P. Van der Voort, *Chemical Communications* 46 (2010) 5085-5087.
- [11] K. Leus, M. Vandichel, Y.Y. Liu, I. Muylaert, J. Musschoot, S. Pyl, H. Vrielinck, G.B. Marin, C. Detavernier, P.V. Wiper, Y.Z. Khimyak, M. Waroquier, V. Van Speybroeck, and P. Van der Voort, *Journal of Catalysis* 285 (2012) 196-207.
- [12] C. Bolm, *Coordination Chemistry Reviews* 237 (2003) 245-256.
- [13] A. Butler, M.J. Clague, and G.E. Meister, *Chemical Reviews* 94 (1994) 625-638.
- [14] T. Hirao, *Chemical Reviews* 97 (1997) 2707-2724.
- [15] A.G.J. Ligtenbarg, R. Hage, and B.L. Feringa, *Coordination Chemistry Reviews* 237 (2003) 89-101.
- [16] Sharples.Kb, and Michaels.Rc, *Journal of the American Chemical Society* 95 (1973) 6136-6137.
- [17] K.B. Sharpless, and T.R. Verhoeven, *Aldrichim. Acta* 12 (1979) 63.
- [18] T. Itoh, K. Jitsukawa, K. Kaneda, and S. Teranishi, *Journal of the American Chemical Society* 101 (1979) 159-169.
- [19] B.E. Rossiter, T.R. Verhoeven, and K.B. Sharpless, *Tetrahedron Letters* (1979) 4733-4736.
- [20] H. Mimoun, L. Saussine, E. Daire, M. Postel, J. Fischer, and R. Weiss, *Journal of the American Chemical Society* 105 (1983) 3101-3110.
- [21] S. Cenci, F. Difuria, G. Modena, R. Curci, and J.O. Edwards, *Journal of the Chemical Society-Perkin Transactions 2* (1978) 979-984.
- [22] R. Curci, F. Difuria, R. Testi, and G. Modena, *Journal of the Chemical Society-Perkin Transactions 2* (1974) 752-757.
- [23] D.E. Babushkin, and E.P. Talsi, *Reaction Kinetics and Catalysis Letters* 71 (2000) 115-120.
- [24] H. Mimoun, *Catalysis Today* 1 (1987) 281-295.
- [25] H. Mimoun, M. Mignard, P. Brechot, and L. Saussine, *Journal of the American Chemical Society* 108 (1986) 3711-3718.
- [26] Y. Hoshino, and H. Yamamoto, *Journal of the American Chemical Society* 122 (2000) 10452-10453.
- [27] K.P. Bryliakov, N.N. Karpyshev, S.A. Fominsky, A.G. Tolstikov, and E.P. Talsi, *Journal of Molecular Catalysis A: Chemical* 171 (2001) 73-80.
- [28] K.P. Bryliakov, E.P. Talsi, S.N. Stas'ko, O.A. Kholdeeva, S.A. Popov, and A.V. Tkachev, *Journal of Molecular Catalysis A: Chemical* 194 (2003) 79-88.
- [29] M. Buhl, R. Schurhammer, and P. Imhof, *Journal of the American Chemical Society* 126 (2004) 3310-3320.
- [30] Y. Nakagawa, and N. Mizuno, *Inorganic Chemistry* 46 (2007) 1727-1736.
- [31] A.E. Kuznetsov, Y.V. Geletii, C.L. Hill, K. Morokuma, and D.G. Musaev, *Inorganic Chemistry* 48 (2009) 1871-1878.
- [32] M.L. Kuznetsov, and J.C. Pessoa, *Dalton Transactions* (2009) 5460-5468.
- [33] Sharples.Kb, D.R. Williams, and J.M. Townsend, *Journal of the American Chemical Society* 94 (1972) 295-&.
- [34] M.V. Kirillova, M.L. Kuznetsov, V.B. Romakh, L.S. Shul'pina, J. da Silva, A.J.L. Pombeiro, and G.B. Shul'pin, *Journal of Catalysis* 267 (2009) 140-157.

- [35] J. Dobler, M. Pritzsche, and J. Sauer, *Journal of the American Chemical Society* 127 (2005) 10861-10868.
- [36] X. Rozanska, and J. Sauer, *International Journal of Quantum Chemistry* 108 (2008) 2223-2229.
- [37] D. Goebke, Y. Romanyshyn, S. Guimond, J.M. Sturm, H. Kuhlenbeck, J. Dobler, U. Reinhardt, M.V. Ganduglia-Pirovano, J. Sauer, and H.J. Freund, *Angewandte Chemie-International Edition* 48 (2009) 3695-3698.
- [38] J.M. Sturm, D. Gobke, H. Kuhlenbeck, J. Dobler, U. Reinhardt, M.V. Ganduglia-Pirovano, J. Sauer, and H.J. Freund, *Physical Chemistry Chemical Physics* 11 (2009) 3290-3299.
- [39] R.A. Sheldon, *Recueil Des Travaux Chimiques Des Pays-Bas-Journal of the Royal Netherlands Chemical Society* 92 (1973) 253-266.
- [40] R.A. Sheldon, J.A. Vandoorn, C.W.A. Schram, and A.J. Dejong, *Journal of Catalysis* 31 (1973) 438-443.
- [41] M.N. Sheng, and J.G. Zajacek, *Advances in Chemistry Series* (1968) 418-&.
- [42] M.N. Sheng, and J.G. Zajacek, *Journal of Organic Chemistry* 35 (1970) 1839-&.
- [43] C.C. Su, J.W. Reed, and E.S. Gould, *Inorganic Chemistry* 12 (1973) 337-342.
- [44] A.O. Chong, and K.B. Sharpless, *Journal of Organic Chemistry* 42 (1977) 1587-1590.
- [45] H. Mimoun, I.S.D. Roch, and L. Sajus, *Tetrahedron* 26 (1970) 37-&.
- [46] A.D. Becke, *Journal of Chemical Physics* 98 (1993) 5648-5652.
- [47] C.T. Lee, W.T. Yang, and R.G. Parr, *Physical Review B* 37 (1988) 785-789.
- [48] M.J. Frisch, G.W. Trucks, H.B. Schlegel, G.E. Scuseria, M.A. Robb, J.R. Cheeseman, J. Montgomery, J. A. , T. Vreven, K.N. Kudin, J.C. Burant, J.M. Millam, S.S. Iyengar, J. Tomasi, V. Barone, B. Mennucci, M. Cossi, G. Scalmani, N. Rega, G.A. Petersson, H. Nakatsuji, M. Hada, M. Ehara, K. Toyota, R. Fukuda, J. Hasegawa, M. Ishida, T. Nakajima, Y. Honda, O. Kitao, H. Nakai, M. Klene, X. Li, J.E. Knox, H.P. Hratchian, J.B. Cross, V. Bakken, C. Adamo, J.J. an, d.R. Gomperts, R.E. Stratmann, O. Yazyev, A.J. Austin, R. Cammi, C. Pomelli, J.W. Ochterski, P.Y. Ayala, K. Morokuma, G.A. Voth, P. Salvador, J.J. Dannenberg, V.G. Zakrzewski, S. Dapprich, A.D. Daniels, M.C. Strain, O. Farkas, D.K. Malick, A.D. Rabuck, K. Raghavachari, J.B. Foresman, J.V. Ortiz, Q. Cui, A.G. Baboul, S. Clifford, J. Cioslowski, B.B. Stefanov, G. Liu, A. Liashenko, P.P. and, I. Komaromi, R.L. Martin, D.J. Fox, T. Keith, M.A. Al-Laham, C.Y. Peng, A. Nanayakkara, M. Challacombe, P.M.W. Gill, B. Johnson, W. Chen, M.W. Wong, C. Gonzalez, and J.A. Pople. 2004. *Gaussian 03*, Revision D.01
- [49] P.J. Hay, and W.R. Wadt, *Journal of Chemical Physics* 82 (1985) 270-283.
- [50] S. Shaik, S. Cohen, Y. Wang, H. Chen, D. Kumar, and W. Thiel, *Chemical Reviews* 110 (2009) 949-1017.
- [51] A. Lundin, I. Panas, and E. Ahlberg, *Journal of Physical Chemistry A* 111 (2007) 9080-9086.
- [52] S. Grimme, *Journal of Computational Chemistry* 25 (2004) 1463-1473.
- [53] S. Grimme, J. Antony, S. Ehrlich, and H. Krieg, *Journal of Chemical Physics* 132 (2010).
- [54] ORCA. 2.8.0ed. <http://www.thch.uni-bonn.de/tc/orca/>.
- [55] V. Van Speybroeck, J. Van der Mynsbrugge, M. Vandichel, K. Hemelsoet, D. Lesthaeghe, A. Ghysels, G.B. Marin, and M. Waroquier, *Journal of the American Chemical Society* 133 888-899.
- [56] A. Ghysels, T. Verstraelen, K. Hemelsoet, M. Waroquier, and V. Van Speybroeck, *Journal of Chemical Information and Modeling* 50 (2010) 1736-1750.
- [57] B. Vlckova, B. Strauch, and M. Horak, *Collection of Czechoslovak Chemical Communications* 52 (1987) 686-695.
- [58] L.J. Bellamy, *The infrared spectra of complex molecules: advances in infrared group frequencies. vol. two.* Chapman and Hall, 1980.
- [59] E.C.E. Rosenthal, H.L. Cui, and M. Hummert, *Inorg. Chem. Commun.* 11 (2008) 918-920.
- [60] S. Vayssie, and H. Elias, *Liebigs Ann.-Recl.* (1997) 2567-2572.
- [61] Vansickl.De, F.R. Mayo, and R.M. Arluck, *Journal of the American Chemical Society* 87 (1965) 4824-&.

Mechanistic insight into the cyclohexene epoxidation
with VO(acac)₂ and tert-butyl hydroperoxide, M. Vandichel,
K. Leus, P. Van der Voort, M. Waroquier, V. Van Speybroeck,
Journal of Catalysis, 294, 1-18, 2012